

SEP 19 1983

CUIMR-T-83-005 C. 3

PELLE LIBRARY

CIRCULATING COPY
Sea Grant Depository

FILE COPY

LOAN COPY ONLY

Side-Scan Sonar Mapping and
Computer-Aided Interpretation of the
Geology of the Santa Barbara Channel

by

Bruce P. Luyendyk, Earl J. Hajic, and David S. Simonett

NATIONAL SEA GRANT DEPOSITORY
PELL LIBRARY BUILDING
URI, NARRAGANSETT BAY CAMPUS
NARRAGANSETT, RI 02882

Department of Geological Sciences

and

Department of Geography

and

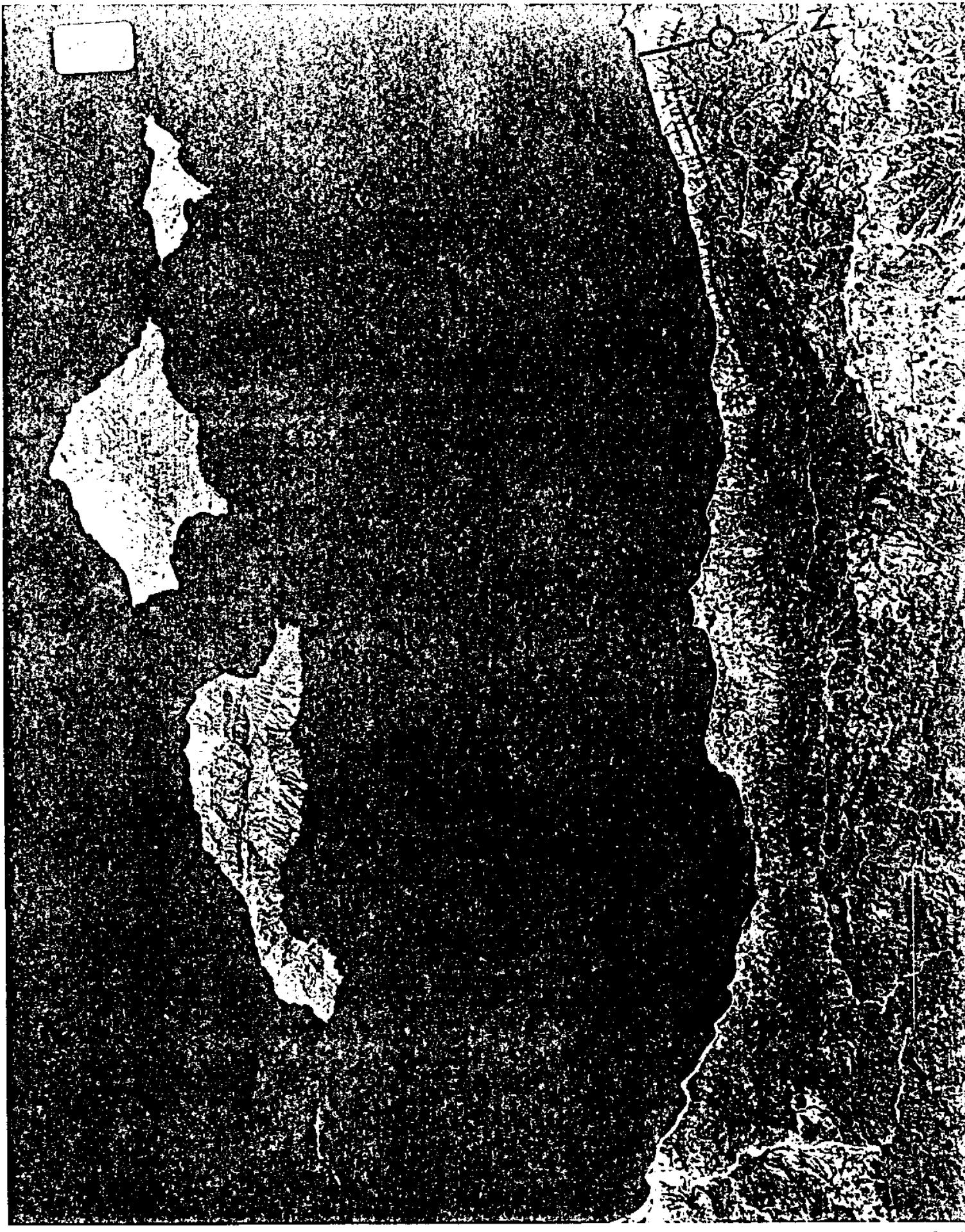
Marine Science Institute

University of California, Santa Barbara

A California Sea Grant College Program Publication

1983

(Luyendyk; R/E-18)



ACKNOWLEDGEMENTS

Many people aided us in all aspects of this project. We have had five Sea Grant Trainees. Tom Powell (now at Union Oil) aided in the logistics of many survey operations. Greg Crandall (now at Hughes Aircraft) aided in field surveys plus developed many navigation computer programs. Robert Crippen (Geography, UCSB) analyzed data from the Cojo Bay and Santa Cruz Channel and produced geologic maps of these areas. Other student help included Jaye E. UpDeGraff (Geological Sciences, UCSB) who processed the majority of the offshore navigation data (Appendix 1), and David Naar (Geological Sciences, UCSB) who developed software for our real-time LORAN-C navigation (Appendix 2). Fred Ennerson (Geography, UCSB) wrote the software for A/D conversion of the side-scan data, digitized the test area and produced the film writer outputs.

Professor W. A. Prothero (Geological Sciences, UCSB) helped us with at-sea logistics and generously shared with us some of his available ship-time.

Assistance from the Marine Science Institute, UCSB, is gratefully acknowledged for purchasing (K. Courtney), accounting (B. St. John, P. Thurston), and administration (F. Ciluaga). The MSI is also thanked for the purchase of the reflection system and LORAN receiver used in our project.

Mark MacLennan, Otto Matt (Geography, UCSB) and Trudy Miller (Computer Center, UCSB) provided computer assistance in some of the early test phases. Joseph Scepan (Geography Remote Sensing Unit, UCSB) and Edwin Gustafson (Geography, UCSB) did the photographic work. Gustafson also drafted the image processing flow chart.

David Crouch (Geological Sciences, UCSB) drafted the majority of our illustrations.

Peter J. Fischer (California State University, Northridge) generously donated his survey data from the Santa Cruz Channel for our use.

Arne Junger of the USGS and UCSB consulted with us several times and provided us data from the Santa Cruz Channel. We are deeply saddened by his recent death.

Finally, the crew of the R/V Ellen B. Scripps is thanked for conducting us safely through the survey areas in the Channel region.

CONTENTS

	<u>Page</u>
ACKNOWLEDGEMENTS	ii
ILLUSTRATIONS	
List of Figures	iv
List of Plates	vii
I. INTRODUCTION	1
I.1 Objectives of seabed mapping	1
I.2 Image processing of side-scan sonar data: Objectives.	2
II. SONAR SURVEYS AND DATA ACQUISITION	6
II.1 Survey equipment	6
II.2 Survey methods and list of cruises	7
Table 1: UCSB sonar cruises in the Santa Barbara Channel region	8
III. DATA PROCESSING	9
III.1 Navigation	9
III.2 Interpretation of 3.5 kHz records	9
Table 2: Offset of LORAN-C positions with respect to latitude and longitude grid	10
III.3 Interpretation of side-scan records	11
IV. IMAGE PROCESSING	11
IV.1 Summary and overview	11
IV.2 A/D conversion: Overview	13
IV.3 Geometric rectification	13
IV.4 Image enhancements	14
IV.5 Stereoscopy and inverse filtering	17
V. RESULTS OF THE MAPPING PROGRAM	18
V.1 Anacapa Passage	18
V.2 Santa Cruz Channel	19
V.3 Naples shelf and slope	20
V.4 Santa Barbara-Ventura shelf	22
V.5 Cojo Bay (offshore LNG site)	23
VI. SUMMARY AND PROJECT EVALUATION	24
VI.1 Geological mapping achievements	24
VI.2 Image processing achievements and evaluation	26
REFERENCES	29
APPENDICES

ILLUSTRATIONS

<u>Figures</u>	<u>Page</u>
Figure 1	
	Survey areas in the Santa Barbara Channel region are enclosed in the numbered boxes in dotted outlines. The larger boxes 6A,B,C are the areas covered in the track compilation sheets. Areas 6A and 6B are given here as Plates 1 and 2. The box labelled SRA is the location selected for a future survey.
Figure 2	
	Side-scan sonar resolution vs. range; adapted from Sutton (1979) and Hajic (1980).
Figure 3	
	Geometry of side-scan sonar insonification and factors which affect image quality. Adapted from Ingham (1975).
Figure 4	
	Lineations in Anacapa Passage which were mapped by digitizing and computer plotting each target.
Figure 5	
	Chart of survey tracks in the Anacapa Passage (Area 1 in Figure 1).
Figure 6	
	Photograph of a portion of the side-scan data taken over truncated dipping beds in Anacapa Passage ("B" in Figure 5).
Figure 7	
	Flow chart of image processing procedures used on sonar data from Anacapa Passage.
Figure 8	
	Elemental positioning grid used to produce geometric rectification of side-scan sonar images.
Figure 9	
	A pair of digital stereo images of truncated beds in Anacapa Passage (vic. 34°N, 119°27'W).

Figure 10
Inverse filter transfer function used to test
image "restoration."

Figure 11
Output image of inverse filter test. Vicinity
34.3°N, 119°29'W in Anacapa Passage (near "A" in
Figure 5).

Figure 12
System modulation transfer function determined
from the outgoing versus returned sonar signal.

Figure 13
Photograph of 3.5 kHz seismic profile across
folds in the Anacapa Passage ("C" in Figure 5).

Figure 14
Photos of side-scan and 3.5 kHz records taken
approximately parallel to strike in Anacapa
Passage ("A" in Figure 5).

Figure 15a,b
Track charts of sonar surveys in the Santa
Cruz Channel (Area 2A, 2B, Figure 1). CSUN
tracks are 3.5 kHz reflection data from California
State University, Northridge.

Figure 16
Track chart of sonar surveys over the Naples shelf
and slope (Area 3, Figure 1).

Figure 17
Line drawing interpretations of 3.5 kHz seismic
profiles over slides on the continental slope off
Naples, California (locations shown on Plate 9).

Figure 18
Line drawing interpretations of 3.5 kHz seismic
reflection profiles taken over the Red Mountain
fault (north branch) south of Santa Barbara
(locations shown on Plate 10).

Figure 19

Photos of 3.5 kHz reflection records taken over the Oak Ridge fault and the buried channel of the Santa Clara River, off Ventura (locations shown on Plate 11).

Figure 20

Chart of survey tracks on the mainland shelf near Cojo Bay, California.

Figure 21

Line drawing interpretations of 3.5 kHz seismic reflection profiles taken across the south branch Santa Ynez fault, south of Sacate, California.

Figure A.1.1

Flow chart of the real-time processing scheme for LORAN-C digital navigation.

Figure A.1.2

Flow chart of the laboratory processing scheme for LORAN-C digital navigation.

Plates

Plates 1 and 2

UCSB geophysical survey tracks in the region of the Santa Barbara Channel. All cruises were made on the R/V Ellen B. Scripps.

Plate 3

Photographs showing a comparison of a shipboard paper copy side-scan sonar record (lower) with the digitally processed version of the same data (upper).

Plate 4

Digital sonar mosaics of a 12 km^2 area of the Anacapa Passage: 4A-geometrically rectified and contrast stretched digital mosaic; 4B-line drawing interpretation of 4A; 4C-low pass and high pass filtered version of 4A; 4D-density sliced version of 4C; 4E-standard deviation filter of 4C.

Plate 5

Structure map of the Anacapa Passage.

Plate 6

First attempt of constructing a digital mosaic for Anacapa Passage (line interpretation of digital mosaic).

Plate 7

Line interpretation of the second version of a digital mosaic for Anacapa Passage.

Plate 8

Structure map for Santa Cruz Channel.

Plate 9

Structure map of the Naples shelf and slope.

Plate 10

Structure map for the shelf south of Santa Barbara.

Plate 11

Structure map for the shelf south of Carpinteria and Ventura.

Plate 12

Structure map for the shelf at Cojo Bay.

I. INTRODUCTION

This report is the final documentation of our Sea Grant R/E-18 which was active from September 1, 1977 to March 31, 1981.

Our goals in this project ran along two parallel but overlapping tracks. One was to map the exposed seabed geology in selected areas of the Santa Barbara Channel using sonar techniques, another was to develop and experiment with computerized image enhancement of side-scan sonar data obtained from our survey areas. Our survey objective was to produce geologic maps of the seabed and to identify geologic hazards such as active faults. Our image processing objective was to use computer techniques to enhance sonar images, to identify features, and to map them in a sonar digital mosaic.

We worked in six survey areas on five cruises during the three years of the project (Figure 1). Sea work was done on the R/V Ellen B. Scripps of the Scripps Institution of Oceanography, in conjunction with seismic monitoring experiments of W. Prothero (UCSB). Our most successful work was done in Anacapa Passage (Area 1) and the Santa Cruz Channel (Area 2A, 2B). We purchased an Edo-Western 606A side-scan system under the grant auspices. Other equipment used included an ORE 3.5 kHz subbottom profiler, a Racal 4-channel FM tape recorder, and a micrologic LORAN-C receiver.

The digital image processing procedures used the VICAR program package developed by the California Institute of Technology Jet Propulsion Laboratory. This software system was originally used for the processing of spacecraft and medical imagery. It was fully implemented here at UCSB largely under the auspices of this project.

I.1 Objectives of seabed mapping

Our purpose in conducting marine surveys was to produce detailed geologic maps of the seabed surface in a few selected areas of the mainland shelf and northern Channel Islands platform. We hoped to explore the utility of side-scan sonar surveying in this region, where, at project initiation, very little if any side-scan work had been done. Thus, in a large sense our objectives were to explore and map. During the last ten years or so high resolution-shallow penetration seismic surveys have been made of several areas on the channel shelf (Mesa², 1978; Ashley et al., 1977; Hoyt, 1976; Greene et al., 1978; Arleth, 1977). To our knowledge, only the Mesa² (1978) study in Cojo Bay utilized side-scan sonar to any degree.

Our main criteria in selecting survey areas were those areas where active tectonic elements (faults, folds) were known or suspected to occur, and/or those areas where little or no high resolution seabed maps were available.

The passages between Santa Rosa, Santa Cruz, and Anacapa Islands were selected for surveying in order to map the traces of major through-going faults. The area of the Santa Barbara-Ventura shelf was mapped to trace major fault zones such as the Red Mountain and Oak Ridge thrusts and also to search for areas of seafloor disruption caused by the August 13, 1978 Santa Barbara earthquake. The survey area south of the Naples shelf (3 in Figure 1) was chosen to study a complex set of submarine slides on the continental slope. The survey area southeast of Point Conception, in Cojo Bay (5 in Figure 1) was studied to search for seafloor features associated with the south branch of the Santa Ynez fault. In addition, the Cojo Bay region is offshore the proposed western LNG (liquified natural gas) storage facility. Therefore our data from here might be useful for informed decisions regarding the seismic safety of the site.

Survey track coverage is shown on Plates 1 and 2 and in Figures 5, 15, 16 and 20 below. Besides the Sea Grant cruises (denoted by SSS prefix) the Marine Science Institute and the Scripps Institution of Oceanography supported cruises MSI-76-1 and MSI-77-1 which also obtained data for this report.

I.2 Image processing of side-scan sonar data: Objective

Underwater imaging is one of the more difficult areas of remote sensing. Water is a medium which is quite unyielding to a wide array of sensors. It is highly opaque to electromagnetic and optical devices, and extremely noisy and turbulent for acoustic sensors. For the latter, the range over which acoustic sensing may be carried out is, at present, relatively limited (see Figure 2 adapted from Sutton, 1979, in which image resolution and range are plotted).

The distinction between conventional sonar and acoustic imaging systems is a difficult one to make. The difference comes from their intended purpose: the goal of a conventional sonar system is to indicate WHERE something is located, while the goal of underwater acoustic imaging is to indicate WHAT it looks like. Medium-range side-scan sonar for most practical purposes is limited to strips some 400 meters wide to the side of the sensor. "Various factors limit the resolutions of both medium- and long-range sonars to about 1/1,000th of the range" (Belderson et al., 1972). Synthetic aperture sonar may be considered to include the holographic acoustic images at the low end of the range scale. Lee (1979) has estimated an azimuth resolution of .5 m for a 100 m to 1,000 m range synthetic aperture sonar using a state of the art processor.

Side-scan sonar equipment (the under-sea analogy of side-scan radar) has been used since 1958 (Ingham, 1975) to map seabed features. It represents a useful addition to seafloor profiling with vertical sounders which employ lower frequency acoustic waves to construct bathymetric profiles and detect subbottom structures.

Conventional side-scan sonar uses a narrow antenna beam (in the plan view) and a wide beam (in the vertical plane) projected at right angles to the track ship or towed "fish." The mapping coverage thus extends from the seabed almost directly beneath a transducer out to the oblique range of the beam (a typical maximum is 400 m). Successive transmissions (e.g., about once every 1/2 second) provide the source for each image line and build up a two-sided view of the adjacent seabed (Figure 3). Completeness and fidelity of coverage depends on ship speed, beam widths, pulse repetition rate, sea state and the effects of yaw, pitch and roll. Whatever the circumstances the record will, however, appear quite normal and give no indication of drift or yaw producing gaps or overlaps in the swept path (Ingham, 1975). For optimum resolution the transducer should be about 1/10 to 1/7 of the full range scale above the seabed. This is achieved in variable depth waters by using a towed "fish" to carry the transducer and signal preamplifiers.

Side-scan sonar image mapping allows a moderate-width swath of seafloor textural information to be obtained in a short period of time through recording both the specular and scattered components of the return signal. Objects in the sonar path, on the order of twenty or thirty centimeters or larger, produce mostly specular (mirror-like) reflections. Thus fault scarps, cracks, outcrops, sandwaves, dunes, and ripples can be recognized. Since scattering of the sonar acoustic signal also takes place, and is proportional to grain size, this potentially allows recognition of differing sediment textures as well (Page and Dyer, 1979) if there is an adequate dynamic range to the signal. If the spatial resolution is appropriate, micro-, as well as meso-scale spatial patterns associated with different grain sizes and deposition environments should, by analogy with radar experience, be detectable (see Figure 3).

The image processing objectives of this study were to digitally enhance the sonar images for improved geologic interpretation by:

1. Employing digital procedures to overcome the problems of dealing with paper analog output: low dynamic range, variable cross, and along-track scale, slant-range rather than equivalent ground-range display, inadequate motion compensation, unsuitability for mosaicking, and cross-track variation in sonar-reflection values.
2. Employing methods of enhancement common in remote-sensing analyses (image sharpening, texture emphasis for enhancement of weak features, overlapping of different-look-angle multi-images to obtain color combination, linear feature detection, and so on) to make the sonar imagery more interpretable for geologic mapping.

3. Assessing the utility of these techniques for sonar imagery and in producing sonar mosaics.
4. Testing the value of sonar stereoscopy in areas of gently sloping submarine topography for improving geologic interpretation.

We had one further objective in addition to the above: to arrange our analyses so that the easier-to-implement techniques were tested earlier. The purpose was to ensure that we did not engage in the more expensive procedures until we were sure of results on the key items: (1) first-order approximate image rectification, and (2) value of image enhancement for detecting substrate differences, enhancing texture differences, weak-feature enhancement, subtle-linear enhancement, etc. These preceded the work on image mosaicking and stereoscopy.

By combining the image processing and geologic interpretation we also proposed to identify a broadly applicable technology and assess the feasibility of developing a transportable technology for improved continental shelf side-scan sonar surveys. This technology and methodology if technically and financially reasonable, would be for potential use in sensitive areas where major geologic hazards exist, submarine exploration and drilling are planned, or where submarine installations are proposed.

Most side-scan sonar research has been severely constrained by the typical output format of paper-tape images. We proposed using a variety of digital processing techniques to make the sonar imagery more valuable for geologic mapping. Sanders et al. (1969) noted that the normal paper-tape display requires considerable experience with its use and much time for interpretation. These factors have detracted from the widespread use of sonar records. The interpretation problems arise from the following:

1. Small dynamic range-frequently almost binary and never better than four gray levels compared to 16 gray levels with film recording. Subtleties of bottom-sediment character are thereby lost.
2. Slant-range display giving variable across-track scale with pronounced near-range image distortion.
3. Differential along and across-track scales.
4. Time-varying along and cross-track scales.
5. Variations in towing-instrument-look angles and directions, producing gaps and redundant scan coverage.
6. Recording system line-dropping.

7. Cross-track nonuniformity in sonar reflections from uniform materials.
8. Discontinuities of the sonar image produced by swell-induced fish path convolution.

Mudie et al. (1970) produced deep-tow side-scan mosaics using variable speed play back of FM recorded data. Berkson and Clay (1973) optically rectified their sonar records. More recently the digital processing of aircraft and spacecraft imagery logically suggested that the same procedures be employed on sonar imagery.

Paluzzi (1976) and Paluzzi et al. (1976) noted that "digital processing of side-looking sonar records is rare; however, Mudie et al. (1970) has (sic) suggested this approach." Paluzzi's own work included the mix of multichannel analog recording of the sonar signals, analog to digital data conversion and the use of the VICAR (video image communication and retrieval) image-processing system at JPL. From that suite of software, he applied geometric corrections, improved contrast ratios, corrected for range-gain changes, and filtered out noise and side-lobe effects (Paluzzi, 1976; Paluzzi et al., 1976). He noted that "a shift in processing emphasis from image correction to information extraction will allow analysts and scientists to pursue large area survey, pattern analysis, grain size and texture measurement from imagery, and automated deposit mapping" (Paluzzi, 1976). In our study, we proposed to engage in this shift from image correction to information extraction.

Clerici (1977) provided an extensive summary of the infelicities in the data collection process forced by the very geometry of ship/fish dynamics. Recently Clerici (1978) introduced and demonstrated a method of evaluating the effectiveness of digital feature enhancement. His thesis was that correlation of independent views of the same imaged area would provide an alternate source of "sea floor truth," which is difficult to obtain, to serve as a reference for such tests. His comparison of correlation values for a selected set of enhancements provides a stimulus for further analyses.

Currently, Dr. C. Lowenstein of Scripps Institution of Oceanography (SIO) has developed a program to digitally process side-scan sonar data from the SIO-MPL deep tow system. His goal is real time display enhancement and backscatter characterization (feature recognition). This Navy-funded project uses an onboard computer, and extends the work reported on earlier by Spiess et al. (1975). EG&G Corporation (Edgerton, Germeshausen and Grier) Clifford (1979) recently introduced equipment with real time digital processing, a dynamic range of <64 db, a 6 kHz sample rate and the display of geometrically rectified and enhanced sonar imagery. An expansive statement in their publicity notes that, "since the data are spatially correct, the location of only one data point (natural feature or man-made) need be known to position the entire mosaic relative to latitude and longitude."

Walker (1978) developed an alternate ground-speed corrected side-scan sonar display system, employing a computer controlled fibre optic face-plate system which transfers the signal appearing on a CRT screen on to ultraviolet (or photo chemical) sensitive paper, thus allowing the production of direct records without any other intervening optical or computer system. This process of direct recording requires precise navigation data, and because it is direct recording, it remains an analog signal, and digital processing is infeasible. It is thus not as preferable an approach as that employed by EG&G, though the latter also precludes further post-hoc digital processing.

Recent equipment developments are precision analog records for phased array, synthetic-aperture imaging, and a dual towed fish configuration for sonar stereoscopy (NTIS, 1977).

Digital image mosaicking employing precise radio navigation has also been reported as a technique by Prior et al., (1979) who evidently were unaware of Paluzzi's (1976) and our (Luyendyk et al., 1978; Hajic, 1980) earlier work and the work in progress. They concluded that "scale-corrected digital side-scan sonar . . . shows promise of allowing significant advances in assessing the spatial distribution of subaqueous failures and their internal characteristics. The ability to observe subtle bottom topography and texture in true dimensions will contribute as much to the field of marine geology as aerial photography did to subaerial topographic mapping."

An important analysis of problems in stereoscopic side-scan sonar has been carried out by Denbigh (1978), who observed that "two side-scan displays taken from different tracks are likely to show a disappointing degree of correlation (in geometry and) particularly in fine structure, and this will greatly impede the visual fusion of the images during stereoscopic viewing." He develops an important procedure, of use in near-range imaging, in which a single-towed body is employed and "stereoscopic images are generated artificially by combining a depth measurement signal electronically with the conventional side-scan signals."

In a recent study, Pace and Dyer (1979), drawing on image processing procedures for texture quantification of side-scan sonar data, also explored the potential of various texture algorithms for clarification and distinction of sedimentary sea-bottom features.

II. SONAR SURVEYS AND DATA ACQUISITION

II.1 Survey equipment

The major survey equipment items used were a side-scan sonar, a high resolution subbottom profiler, and a LORAN-C navigation receiver.

The side-scan transceiver is an Edo-Western model 606A which operates at 100 kHz and 1.5 kw with a pulse length of 100 microseconds. Normally we surveyed using maximum range settings of 400 meters (0.53 sec rep rate) but sometimes we used 200 meters range (0.27 sec rep rate). We had the transceiver modified so that the analog signal output to the dry paper was available at output jacks. The left channel, right channel and synch pulse were recorded on separate tracks of a 4-channel Racal FM tape recorder. This was the data source for our image processing procedures. The side-scan tow body is an Edo model 603. The transducers were made specially to operate to depths of 2000 meters, although during our work the tow fish never reached below 50 meters. The system was controlled via a hand winch equipped with slip rings. The tow body also housed an Edo pressure-depth sensor during our later surveys.

The profiling system used is an ORE model 136 reflection system. This was driven at 3.5 kHz by an ORE model 140 10 kw transceiver. The data were recorded on a Hydroproducts Giffit 4000T dry paper 19 inch recorder.

Fortunately for us, the LORAN-C navigation network became active at the beginning of our project. We used a Micrologic ML-1000 receiver. This unit was modified and interfaced to a North Star Horizon II microcomputer and a Houston omnigraphic flatbed plotter to provide a digital navigation log and to produce ship's tracks in real time on later cruises.

II.2 Survey methods and list of cruises

A survey operation typically involved towing both the side-scan and a 3.5 kHz fish at 5 knots on a grid pattern with 200 to 500 meter spacing. The 3.5 kHz fish was towed at a depth of 8 meters just off the stern and the 603 side-scan fish was towed about 25 to 35 meters off the seafloor where possible. The LORAN antenna was attached to the stack of the E. B. Scripps. LORAN fixes were recorded every 15 minutes on our first trip, then at 5 minute intervals on later ones. This time interval proved too large for sonar mosaicking and on our last trip we took navigation fixes every 21 seconds. This was accomplished by using the North Star Horizon II microcomputer and writing each fix to disc automatically. Radar fixes were taken simultaneously during the surveys at 15 to 30 minute intervals. Positioning of the ship's track by radar served to calibrate the LORAN fixes in given areas to allow for local refraction effects. During the surveys the side-scan data was analog recorded on magnetic tape. We had problems with the signal-to-noise ratio on the recordings for our earlier surveys but our last recordings were made on the Racal 4-channel unit, and these data are excellent.

Data summarizing cruise activities since 1976 are given in Table 1. Side-scan data were successfully tape recorded only

Table 1

UCSB Sonar cruises in the Santa Barbara Channel region

Cruise	Dates	Areas	SSS	3.5 kHz	FM Tape	Digital Navigation
MSI-76-1*	11/16/76-11/18/76	Santa Barbara (4B)		X		
MSI-77-1*	05/23/77-05/25/77	Santa Barbara Channel and 4A + 4B		X		
	05/26/77-05/27/77	Point Conception and Point Arguello		X		
SSS-77-1	11/03/77-	Santa Barbara and Ventura (4A + 4B)	X**	X		
	11/03/77-11/04/77	Cojo Bay (5)	X**	X		
	11/08/77-11/09/77	Anacapa (1)	X**	X		
	11/09/77-	Santa Cruz (2)	X**	X		
SSS-78-1	05/31/78-06/01/78	Anacapa (1)	X	X		
	06/01/78-06/02/78	Naples (3)	X	X		
	06/03/78-06/04/78	Santa Cruz (2)	X	X		
	06/04/78-	Ventura (4A)	X	X		
SSS-78-2	07/21/78-07/22/78	Cojo Bay (5)	X	X		
	07/23/78-	Santa Rosa (SRA)	X	X		
SSS-79-1	11/27/79-	Santa Barbara (4B)	X	X		X
	11/28/79-	Anacapa (1)	X	X		X
SSS-80-1	07/21/80-	Santa Barbara (4B)	X	X		X

*Satellite and radar navigation only

**Starboard side-scan channel dead for this cruise

on SSS-79-1. Consequently this is the data base used for the image processing described in this report.

III. DATA PROCESSING

III.1 Navigation

Ship and fish positions are a critical data base for our project. We have attempted to mosaic side-scan data from Anacapa Passage (below) using automated registration of digital images. Because the spatial dimensions of recognizable features can be as small as one meter, this is also the required precision of the navigation data base. Using LORAN-C we obtained a precision of about 100 meters. Clearly this navigation method lacks the required precision; however, LORAN-C proved excellent for detailing maneuvers of the ship as a fix is calculated every 23 seconds. In the mosaicking process we used the LORAN navigation base to locate the sonar tracks relative to one another, then by hand selected matching features on adjacent sonograms and assigned them common ground points (discussed later).

The navigation data bases were processed via two different schemes. For cruises SSS-79-1 and SSS-80-1 fixes were digitally acquired and logged every 23 seconds. These raw fixes were then edited and smoothed to produce a one minute interval navigation series (Appendix 1). LORAN-C fixes were recorded by hand on SSS-77-1, 78-1 and 78-2. Fix interval was 15 minutes on 77-1 and 5 minutes on the others. The hand-recorded data was processed and checked in a time-consuming method of plotting, editing, re-plotting (Appendix 2). The hand-recorded data were fraught with many transcription errors and omissions which required laborious attention after the fact.

In all our survey areas we found that the LORAN-C navigation net was systematically offset from the map grid. We statistically determined the offset in each area and corrected the LORAN-C navigation base to the map grid. The offset was determined by acquiring radar fixes at 15 or 30 minute intervals and at times synchronous with the LORAN fixes. The offset is defined as the Radar latitude or longitude, minus the LORAN latitude or longitude; therefore a positive offset indicates the LORAN latitude is too far south or the LORAN longitude is too far west. Table 2 shows that LORAN latitudes are about 0.3' too far south in the northern and eastern regions of the channel and about 0.5' to 0.7' too far south in the Santa Cruz and Santa Rosa region. LORAN longitudes are offset slightly east in the eastern end of the channel and offset about 0.3' west in the western channel.

III.2 Interpretation of 3.5 kHz records

All reflection records were analyzed by visual inspection for key features. Geologic features which were found and mapped include folds, faults, buried and to the seafloor, active and

Table 2

Offset of LORAN-C positions with respect to latitude and longitude grid

Area	Cruise	Lat. Offset*	Long. Offset*
Anacapa	SSS-77-1	0.37' \pm 0.21	0.12' \pm 0.62
	SSS-78-1	0.32' \pm 0.26	0.07' \pm 0.15
	SSS-79-1	0.37' \pm 0.24	-0.09' \pm 0.43
Santa Cruz	SSS-78-1	0.55' \pm 0.18	0.18' \pm 0.16
Naples	SSS-78-1	0.35' \pm 0.14	0.32' \pm 0.18
Ventura	SSS-78-1	0.45' \pm 0.13	-0.06' \pm 0.7
Santa Barbara	SSS-77-1	0.35' \pm 0.29	-0.17' \pm 0.48
	SSS-79-1	0.35' \pm 0.12	-0.14' \pm 0.14
	SSS-80-1	0.29' \pm 0.02	0.02' \pm 0.15
Cojo Bay	SSS-77-1	0.34' \pm 0.15	-0.26' \pm 0.19
	SSS-78-2	0.37' \pm 0.09	0.31' \pm 0.16
Santa Rosa	SSS-78-2	0.74' \pm 1.17	0.09' \pm 1.52

*Add these values to uncorrected LORAN fixes to obtain map positions;
 \pm value is one standard deviation.

abandoned channels, erosion surfaces, terraces on the shelf, outcrops of acoustic basement, and areas where little or no Holocene sediment has accumulated. Side-scan data was used to link two-dimensional features seen on adjacent tracks. The highest quality reflection data was obtained from the Anacapa survey area and the Santa Barbara-Ventura shelf.

III.3 Interpretation of side-scan records

Side-scan records were visually interpreted in terms of textures and lineations. Faults, truncated folds, trends of bedding, outcrops, and areas of sediment movement and scour were easily recognized in most cases. The best side-scan records were obtained from Anacapa Passage and Santa Cruz Passage.

All of our digital image processing efforts on side-scan data were concentrated on two data sets from Anacapa Passage. This work is described shortly. In addition, we experimented with processing side-scan features by using a digitizing table. The data base for this work were SSS-77-1 records from Anacapa Passage. Because the dry paper side-scan records are electrically conductive, they could not be digitized directly on the table. Instead, we first traced features in 15 minute blocks onto drafting paper. Faults, bedding, and outcrops were discriminated. The digitizer wrote these data plus the fish (side-scan) height as a disc file on the campus computer. This file was then merged with the matching navigation file to produce a slant range and ship speed-corrected map of bottom features (Figure 4).

IV. IMAGE PROCESSING

IV.1 Summary and overview

The image processing procedures have undergone a long evolution of testing to determine the optimum processing flow. Major problems were encountered handling the sheer volume of the sonar data. In our latest efforts the analog data were digitized at 1.62 kHz and 13 bits in our computer lab (Figure 7). These data were then condensed by a two-sample average and converted to 8 bits. The digitized data were divided into sub-images which were about one-half hour long. Each sub-image contained 3000-4000 scans per side (port and starboard), and 226 samples in range per side after another two sample average. Each sample or pixel represents 1.77 meters in range and was assigned a gray level value from zero to 255 (8 bits) where zero is black. The sub-images were then geometrically rectified to convert time and range data to ground coordinates. This requires the input of sonar depth and navigation series to construct geometric control grids for the sub-images. After rectification the sub-images were filtered and/or contrast stretched. This operation enhances the contrast in the sub-image. Also, the images were processed to reduce noise and to enhance edges. Beyond this step two basic directions were taken.

One approach was to perform automatic and manual feature correlation between separate sub-images and then to overlap these data into a new mosaicked data set. The mosaicked data set was then output onto a negative via a film writer. Another approach was to experiment with sub-image restoration via inverse and Wiener filters. Additionally we attempted to produce a stereo image from enhanced sub-image pairs. This was not successful because navigation control was not precise enough to permit accurate stereo registration, and also the signal quality of the overlapping pairs was too poor. From our experimentation with image processing we learned that two relatively straightforward steps produce dramatic image improvement. These are geometric correction (rectification) for slant range, ship's speed and course change, and contrast stretching. The process and results of these procedures are described below.

All digital image processing was accomplished on data sets from the Anacapa Passage. We visited this region on three cruises (Table 1 and Figure 3). On the first two trips we attempted to record the sonar data on an FM-FM analog recorder. This proved unsuccessful on both trips and yielded a signal-to-noise ratio (S/N) of one, or less. On SSS-79-1 we obtained high quality FM recordings with our Racal unit. Anacapa Passage proved an ideal test area for our sonar image processing because of the dramatic seafloor features present there. In the Passage are an east-west trending anticline and syncline which are truncated at the seafloor, exposing a linear pattern of resistant ridges (Figure 6). The side-scan data set largely consists of one feature type, lineations or ridges, cut at high angles by left-offset faults. These features offer a good opportunity for feature recognition on adjacent tracks.

Our image processing goals were to increase sonar image quality beyond that present on the original paper records and to produce a digital mosaic of separate sonar images. All of the processing reported here was done on the SSS-79-1 data set from Anacapa Passage (Figure 5). The sonar data was separated into nine individual east-west tracks each including about one-half hour of data. For each track separate images were initially defined for north-looking and south-looking sides. Thus a total of 18 separate images for the area (each including about one-half hour of sonar data) were input for the image enhancements and mosaicking.

Data volume is an important concern in the image processing flow. Since data volume significantly influences the feasibility of all the desired image processing, a major initial decision was to define a reasonable digital pixel spatial size. Considering the A/D sampling rate of 1.62 kHz and the system noise, a data volume reduction by a factor of four was considered reasonable. This

was effected by a 2 pixel average done twice in the cross track direction; once before extraction of the synch pulse and once after image formatting (Figure 7). This reduced the 3 1/2 Mega byte data sets of each of the 400 meter range north- or south-looking survey tracks to about .9 M byte. Reduction of the total data volume from the initially digitized 70 M bytes to some 17 1/2 m bytes now placed processing times and costs and data storage requirements in a more reasonable range.* A typical primary image was then 3000 to 4000 lines by 226 samples per side. The pixel size was 1.77 m for the 400 m range tracks and .44 m for the 200 m range tracks. The 200 m range tracks were also averaged over 2 lines besides the 4 sample averaging.

IV.2 A/D conversion: Overview

The port, starboard, and synch pulse signals from the 606A side-scan were recorded on three separate channels of a Racal FM tape recorder. Digitization of the FM records consisted of performing A/D (analog to digital) conversion on small overlapping segments from each track of data. Each of these segments was transferred to the Computer Systems Lab PDP 11/45 to be reconstructed. The first step of reconstruction consisted of separating the port, starboard and synch channels (see image processing flow diagram, Figure 7). The second step was to manually locate the synch pulse in the synch channel using an interactive graphics system. The third step created an image file for each segment. The fourth step mosaicked all of the small images into one large image (i.e., the entire half hour track of data). Each track (port and starboard) was checked to make sure it was processed correctly. If it was, each track was written onto tape for further processing on the ITEL AS/6 campus computer. The details of the A/D process are more fully described in Appendix 3.

IV.3 Geometric rectification

Geometric rectification is the conversion of sonar data as a function of time down range and time along track, to data as a function of latitude and longitude (X, Y). A "two-pass" geometric rectification procedure was used - the first pass corrected for slant range and ship-fish longitude variations; the second corrected the track for the latitude variation. Sonar fish height was determined at 1 min interval sample points from the original sonar image data. Selected image "flips" (rotations) were necessary to render data sequences compatible with fish towing direction or image geometry (Figure 7). The geometric corrections were initially based on navigation data interpolated to 1 minute intervals. A 350 control point grid (see Figure 8 for a 1 min elemental portion) was used on the first rectification pass for each side (port and starboard) of each ship track. Each control

*For comparison, a typical 4 channel Landsat image of a 185 by 185 km scene is about 28 M bytes. This is a rather formidable image processing data volume even in contemporary practice.

point in the grid specified the line and sample positions of the input and output (rectified) pixels. A 120 point grid was used in the second rectification. This second correction, based on the 1 minute interval navigation data input produced "first-cut" sonar tracks for computer and manual mosaicking and evaluation. The 18 separate track images and 2 computer mosaicked images were then written on the film writer. Enlargements from the film transparencies were used for common feature identification. This allowed refined inputs for subsequent geometric corrections and mosaicking.

An initial goal was to produce separate north-looking and south-looking mosaics so that each sonar mosaic would have a common illumination direction. This was abandoned when preliminary mosaicking revealed that the actual ship tracks had not provided the desired overlaps. The revised goal was one mosaic comprised of both the north- and south-looking sonar images. The tradeoff considered that image interpretation would be helped more by "full scene coverage" than hindered by the alternating illumination/shadow directions.

The necessity of an iterative manual-computer mosaicking sequence, while anticipated, became even more obvious after viewing the first mosaic. Common features, identified on separate tracks, were generally misregistered by distances significantly greater than those forced by the irregular corrections of the 1 min navigation data. This misregistration was undoubtedly due mainly to imprecise navigation data. Thus the navigation data was further smoothed by fitting a second or third degree polynomial to the navigation points and the two geometric rectification passes were repeated. We further accommodated the navigation errors by visually inspecting adjacent overlapping sonar tracks for common features. Once these features were identified in common, a new third set of rectification grids was specified and a new mosaic produced. For this second mosaic 25 control points of common features defined revised 120 point grids for each track. For this second computer-generated mosaic, common feature displacement errors still exceeded 150 meters rms (85 pixels or more).

The third and final corrected mosaic was effected by further speed and latitude corrections to tracks 10 and 12 and revised mosaic track positions for tracks 14, 10, 12 and 8 using track 9 as a reference.

IV.4 Image enhancements

Two major types of enhancements were evaluated. These were (1) a variety of contrast stretches, and (2) combinations of low and high pass filtering. Conventionally, contrast enhancement is the final process after both geometric corrections and image filtering. For comparison purposes, however, one set of tracks was contrast stretched immediately after the geometric rectification

and then mosaicked (Plates 3 and 4A). Though the extremes of the gain changes are highly evident, these images provide for useful geologic interpretations when used in conjunction with a more processed set. The dramatic improvement in sonar image quality by geometric rectification and contrast stretching is displayed on Plate 3. Here the lower panel is a photo of the original dry paper sonar record taken on a west-to-east track in the Anacapa Passage. The upper panel is the sonar image produced from the FM tape of the same data. This image has undergone a minimum of processing: A/D conversion, 2-sample cross and along track averaging, geometric rectification, and contrast stretch (Figure 7). The processed image reveals exposed beds of a truncated fold and sediment patterns, which are all but invisible on the original records.

Another image processing experiment used low and high pass filtering in sequence followed by contrast stretch (Plate 4B). The low pass filtering was primarily to improve the S/N ratio. Several filter sizes were evaluated using NLW (number of lines width) equal to 3 or 5 and NSW (number of samples width) equal to 3 or 5. Both averaging (i.e., mean DN* value) and median low pass DN filters were evaluated. The selected median low pass filter has recently found use because of its preservation of sharp edges; hence it is often used to smooth images before applying an edge operator (see, e.g., Narendra, 1981). Because of its nonlinear nature, however, median filters "defy characterization in the spatial frequency domain."

High pass filtering was used primarily to remove the obvious range-gain "banding." This banding is displayed as a white reflective area immediately adjacent to the sonar fish or track center line (Plate 3). Ideally, range gain changes would be compensated for before latitude geometric corrections (when range is simply related to image sample position). However, the pragmatics of images with differing (north and south) range-gain functions which were also occasionally changed during the mapping precluded such a simple solution.

An alternate, and approximately equivalent, solution was sought by implementing a high frequency signal gain correction algorithm logarithmically related to the amplitude of the local image low frequencies (i.e., the range gain trend). Some 25 different functions evaluated failed to produce satisfactory results throughout all range portions of the image.

The preferred method of eliminating the range gain banding used a high pass filter of NLW equal to 121 lines and NSW equal to 1 sample. Other combinations evaluated used NLW values of 15, 31 and 61 lines and NSW values of 1, 3, 5, 15, 31 and 61 samples. A low value of NLW effects range gain compensation even during relatively large ship course changes (i.e., when constant track

*DN = data number; the value between 0 and 255 assigned to a pixel to represent its grey value, from 0 (black) to 255 (white).

range occurs at rapidly changing image sample values). However, it severely suppresses all linear features approximately parallel to a constant sample position. This suppression would eventually include the cross section of linear features at other orientations as well. At the other extreme, a filter with a large value of NLW preserves most linear features at a relatively constant sample position but produces artifacts arising from rapid course changes.

Both mean (linear) and median (nonlinear) high pass filters were evaluated. The significantly higher cost of the median filter at the required large line width and its overemphasis of the low pass median filter effect on the image favored the simple, mean high pass filter. In our example, the individual tracks were low pass filtered, mosaicked and only the mosaic high pass filtered.

A comparison of the unfiltered vs. filtered mosaics (Plate 4A vs. 4C) shows that textural information is largely suppressed in the filtered image. Also, the filtered image shows a bolder display of lineations. The range-gain band is removed in the filtered mosaic and some details are easier to discern within it.

The filtered mosaic was contrast stretched before being additionally processed into a "binary image." The object of producing this image was to enhance lineations and further attenuate textural information and high frequency noise. The binary image (Plate 4D) was produced by simple density slicing of the low pass-high pass filtered image at a DN level of 100 (i.e., all DN values from 0 to 100 were set equal to 0-black; all other values above 100 were set equal to 255-white). Two other density slicing levels (43 and 68) produced inadequate features in the far range locations of the individual tracks. An alternate method of producing the binary mosaic would have used a mosaicking program that summed the individual filtered, density sliced tracks. Two aspects precluded its use: (1) without precise track registration significant "noise" is added to the mosaicked product due to misregistration, and (2) the almost complete overlap of some of the ship tracks prevented the desired effect of the higher gain, near range regions of one track reinforcing the low gain, far range regions of another track; i.e., high gain regions overlap as do low gain regions.

Comparing 4C and 4D shows no appreciable improvement in lineation recognition for density slicing on this image.

Another edge enhancement experiment we performed was to compute a standard deviation image (Plate 4E) from the filtered image (4C). This process is sensitive to rapid lateral changes in contrast. The image is computed by finding the DN standard deviation in a moving 5 x 5 pixel grid. The values of standard deviation found are then contrast stretched over the DN range 0-255. The deviation image (4E) shows much fine lineation detail.

It even enhanced areas of rough bottom near 34°N, 119°29.5'W. We refrained from producing a standard deviation mosaic from the unfiltered image (4A) because we expected that mosaic to contain too much high frequency noise which would lead to additional spurious or false lineations.

The side-scan sonar imagery in the Anacapa Passage shows that the primary bottom features are lineations. In Plate 4B we show a lineation interpretation of mosaics 4A and 4C which was constructed by hand. Also shown on 4B is the geologic structure, which is discussed in section V.1. The lineation information is best extracted through the standard deviation mosaic (compare 4B and 4E). The mosaic shown on 4E could be improved if the survey tracks had been properly accomplished to provide 50% overlap. Ocean current vorticity in the Passage during SSS-79-1 prevented this. With properly overlapping images individual tracks could be summed so that high gain range information could boost low gain regions. This would eliminate the data gaps evident in Plate 4E.

IV.5 Stereoscopy and inverse filtering

Significant amounts of intentional overlap occur in several track pairs. This fact offered the possibility of experimenting with stereo viewing of the sonar features. The sub-image selected for a stereo pair used tracks 8 and 9 (Figure 9). The pair was produced from images with low pass median filtering and an equal DN-area contrast stretch prior to the film-write transparency. The large feature in the lower left (SE) of the image pair seemed a preferred test region because of apparent shadowing differences. Other image regions (for example, other portions of this stereo pair) do not suggest the stereo effect. Even this particular image does not lend itself well to a stereo view. The main difficulty is feature misregistration due to navigation imprecision. Presumably, if navigation precision could be improved, stereoscopy would be possible with sonar images made from the same look direction, as is now done with precisely navigated radar images.

Inverse, or Wiener filtering, seeks to restore an image by incorporating a priori information describing the approximate system signal/noise ratio and a point spread or transfer function. The latter would presumably include the effects of the turbulent medium. In the absence of specific information about the point spread function in a given area, an alternate frequently used is to define the grey values as a Gaussian shaped spot. A point spread function image was generated using a one pixel-wide standard deviation in both the line and sample directions of the image. Additionally, an S/N ratio of two was used. This was based on a reasonable average of the signal characteristics over about the closest 2/3 of the total slant range - at farther ranges the S/N quickly decreased to a value of one or less.

The combined effect of this point spread width and the S/N ratio results in the inverse filter transfer function shown on Figure 10. Features with frequencies below 0.2 cycles/sample are approximately unchanged and those above this frequency are significantly attenuated. Using a higher S/N ratio would cause the transfer function to have a higher peak occurring at relatively higher frequencies. A 512 line x 512 sample image processed with the function in Figure 10 is shown in Figure 11. Some improvement was apparent.

In an earlier experiment we attempted to determine the point spread function via the transform of the system modulation transfer function which we measured (Figure 12). We computed the spectral characteristics of a significantly sharp imaged edge (as recorded on the FM tape and subsequently digitized at a 6 kHz rate). That modulation transfer function was quite broad with half-power near 1.5 kHz, or between 0.2 and 0.3 cycles/sample. Undoubtedly, the imaged edge and hence the system modulation transfer function contained the effect of significant environmental noise. This was one of the reasons for subsequently reducing the digitizing sampling rate and performing cross track sample averaging.

Generally, inverse filtering (image restoration) is not a cost-effective operation for our sonar data considering the uncertainty in describing the actual system point spread function and the low S/N.

V. RESULTS OF THE MAPPING PROGRAM

V.1 Anacapa Passage

The Anacapa Passage is a flat shelf of the northern Channel Islands located between the east tip of Santa Cruz Island and the west tip of west Anacapa Island (Figure 1). The Passage has a depth of about 20 fathoms or more and covers 25 sq. n. mi. (Figure 5). The Passage has been planed flat during a marine transgression exposing the Miocene Monterey formation. This formation also crops out to the west on eastern Santa Cruz Island. To the east on Anacapa Island, the Miocene Conejo volcanics are exposed; this formation is stratigraphically lower than the Monterey (e.g., Greene et al., 1978).

We mapped the Passage in three surveys on SSS-77-1, SSS-78-1 and SSS-79-1. In the Passage we found a large anticline-syncline pair in the Monterey formation (Plate 5). These folds have been truncated at the seafloor (Figures 13 and 14). The exposed resistant ridges of the Monterey provide excellent sonar targets. Offsetting the fold axes are at least three NE-SW trending left-offset (slip?) faults which are also clearly seen on side-scan sonar (Figures 6 and 14). A much more complex area of faults and folds was mapped in the northwest area of the Passage.

East-west trending faults with normal separation bound the Passage, suggesting it represents the top of a horst. The truncated folds are devoid of any appreciable Holocene (?) sediment cover except north of a boundary fault near 34°01'N. On the south edge of the Passage platform a prominent set of north-side-up faults were mapped (Plate 4). These faults appear quite significant in scale and are possibly the trace of the Dume-Santa Monica fault zone mapped farther east. Also, these faults probably connect with the Santa Cruz Island fault to the west although we did not survey their westward continuation (see also, Junger, 1979). A 4.5 M earthquake was located at the base of the Passage south slope in 1973 (see Greene et al., 1978).

The structure of the Anacapa Passage appears to reflect NE directed compression which began in the Channel Islands region in Pliocene time. Left-oblique motion on the Santa Cruz-Dume fault system suggests that the NE-SW faults mapped in the Passage are left-slip Riedel shears.

In section IV we discussed the image processing of side-scan data from the Passage. In Plate 6 we have reproduced at 1:24,000 scale the line interpretation shown in Plate 4. Also, Plate 7 is a line interpretation of an earlier sonar mosaic made from data obtained on SSS-77-1 and SSS-78-1. The line interpretations can be compared directly with the structure map (Plate 5). South of 34°01'N the east-west trend of the truncated beds is readily apparent as is the core of the truncated syncline. Both sonar mosaics show this well, but Plate 6, based on better sonar data and navigation, is the more accurate. The east-west anticline, plus the complex folds to the NW are very obscure on the sonar mosaic interpretations. These structures were located primarily by interpretation of the 3.5 kHz reflection data. The pattern of the truncated beds for both the anticline and syncline shows that these structures plunge to the east.

V.2 Santa Cruz Channel

In the Santa Cruz Channel we combined data from three surveys to construct a structure map. These surveys included SSS-77-1 and SSS-78-1 plus CSUN-75 (Figure 15). The last survey was conducted by Dr. P. J. Fischer of California State University, Northridge. Side-scan data were obtained on SSS-77-1 and 78-1, and 3.5 kHz reflection data were taken on all three. The channel is about 20 fathoms deep, 5 n. mi. wide and covers an area of about 35 sq. n. mi. Miocene volcanic rocks and the Miocene Blanca formation crop out in places on the channel floor (Junger, 1979).

In the area west-northwest of Frazier Point (west end of Santa Cruz Island) a large northwest-plunging anticline has been found (Plate 8). This feature, mapped over an area of at least 18 square kilometers, has not appeared in available previous

mappings (Junger, 1976, 1979). The apparent reason for this is that it is largely obscure in subbottom profiles. The inclusion in this study of side-scan sonar imaging of the sea bottom has allowed us to map out curvilinear ridges protruding through the Holocene surficial sediments. These ridges are the topographic expression of the structure and thus can be used as a surrogate in its delineation. To the south of the anticline, a general change in morphology and the lack of evidence of the anticline are consistent with an extension of the Santa Cruz Island fault northwest about 15 km into the channel. Considering that the Santa Cruz Island fault displays left-offset, it is apparent that the anticline we mapped may be the missing northwest half of the Christi Anticline located in southwest Santa Cruz Island (Weaver et al., 1969). This anticline consists of Paleocene, Eocene and Miocene strata which were folded during latest Eocene to early Miocene time. Its mapped offset in the channel suggests 10 kilometers of left slip since the folding occurred. On the other hand, we mapped a submerged sedimentary terrace which crosses the fault near $120^{\circ} 01'W$ (Plate 8) which is not noticeably offset. (This same sedimentary terrace is found again off southeast Santa Rosa Island).

In contrast to the relatively thick (typically 6 m), discontinuous Holocene sediments located between the ridges of the topographically expressed anticline in the northwest channel, deposits to the south of the inferred fault zone are commonly extensive but thin. In many cases the deposits cannot be distinguished in the subbottom profiles, yet they clearly blanket the surface as seen in the side-scan records. A thickness of less than 2 meters is therefore inferred. A few faults and folds have been discovered beneath the deposits and additional inferred faults are expressed topographically.

The Santa Rosa Island fault is quite clearly expressed on the channel floor. It includes at least three faults with alternately north and south facing scarps a few meters high. The fault zone apparently truncates a NW-SE trending submarine canyon which trends towards Santa Cruz Basin. The Santa Rosa Island fault clearly trends east to abut against the Santa Cruz Island fault - a relationship previously noted by Junger (1976). The geometry of this relationship is puzzling for wrench faults and was discussed by Junger (1979). Both the Santa Cruz and Santa Rosa Island faults are interpreted by him to be major left slip faults. If so, a complex history must be designed to account for the apparent truncation of one fault by another. Some of this history may include dip separation not widely recognized.

V.3 Naples shelf and slope

The Naples study area lies between $119^{\circ}54'W$ and $120^{\circ}05'W$

(Figure 1) and spans most of the continental slope here. One cruise (SSS-78-1) was conducted here to study in more detail submarine slides mapped on the slope by Vedder et al (1974) and later by Yerkes et al. (1981), among others. The geology of part of the adjacent shelf has been presented by Ashley et al. (1977). Side-scan data was not useful because the fish was only briefly within insonification range of the seafloor. The 3.5 kHz data obtained revealed a complex pattern of slides, slumps and slide scars (Figure 16 and Plate 9).

Chaotic slides are found below the 200 fm contour and extending well out into the Santa Barbara Basin floor. At least 6 separate slide units can be recognized and mapped between tracks (Figure 17). Other mass-movements have occurred here without internal disruption of the sediment package. Two or three of these slides or slumps have been mapped farther up the slope above the chaotic slides (Plate 9 and Figure 17).

The origin sites for the slides appear as a band of thinned or missing sediment section between the 100 and 200 fm contour. The area of these origin sites is apparently much less than the slides. Also, one origin site appears to occur on top of a slide (Plate 9). This suggests that the mapped origin sites for mass-wasting are relatively younger than most of the slides.

Although the assignment of relative ages to the slides is fairly straightforward, it is a more difficult matter to assign absolute ages to them. All the slides appear covered by significant thicknesses of sediment. Some slides have served as tectonic dams to downslope sediment movement. Because the rate of sedimentation on the slope is highly variable, use of sediment thickness atop slides to estimate age is questionable. The younger (upslope) slides appear to be covered with about 5 or 10 meters of sediment. Soutar and Crill (1977) determined sedimentation rates in the Santa Barbara Basin of around one meter per 500 years - this is a reasonable upper bound for slope sedimentation rates. Assuming this rate, the youngest slides are around 2500 to 5000 years old, or post-Holocene transgression.

In this vein, apparently we have not mapped any slide associated with the 1812 Santa Barbara Channel earthquake which had an estimated magnitude of M7 (see discussion in Yerkes et al., 1981). If the youngest (highest) slide was associated with this event, then a sedimentation rate of one meter per 20 or 30 years is suggested.

However, the possibility still exists that these separate slides are earthquake-generated. This is particularly plausible considering that the U. S. Geological Survey (Yerkes et al., 1981) has recently proposed that the north mainland shelf is bounded by an active north-side-up reverse fault - the Arguello north channel slope fault system.

V.4 Santa Barbara-Ventura shelf

This portion of the mainland shelf has been extensively mapped, mainly in the subsurface, by several petroleum companies. Almost all of this data is proprietary but some of it has made its way into government reports (Vedder et al., 1969; USGS, 1975; Campbell et al., 1975; Standard oil, 1976; Greene et al., 1976), theses (Hoyt, 1976; Jackson, 1981), and other publications (Curran et al., 1971).

Our work on the shelf used both side-scan and 3.5 kHz reflection, but the sea bottom is relatively featureless, rendering the side-scan data largely uninformative.

Our mapping results show mainly the surficial geology (Plates 10 and 11; tracks shown on Plate 1). On the maps our interpretations are shown in heavy lines while map interpretations of other workers are shown dotted. There are some striking disagreements in the mapped traces of faults and in assigning names to certain faults and folds.

We found that the shelf between Goleta and Rincon Point is dominated by an abrupt step in the seafloor which displays a curvilinear trend. We interpret this feature to be a southside-up reverse fault - the vertical seafloor separation on this fault reaches 10 meters and it probably offsets Holocene materials (Figure 18). South of this fault we found two other southside-up faults, which offset the buried erosion surface, but may or may not offset the present seafloor. The northernmost fault is 18 n. mi. (33 km) long, the next one farther south is 5 n. mi. (9 km) long, and the southernmost is 12 n. mi. (22 km) long. The northern and central faults are associated with the flanks of folds. The central fault may be a faulted anticlinal crest (Figure 18). The northern fault is associated with a seafloor swell which is devoid of sediment (Figure 18, Plate 10).

We have called the northern fault the Red Mountain fault (north branch) after Hoyt (1976). Jackson (1981) places the Red Mountain fault much farther north, near latitude 34°23'N between Santa Barbara and Carpinteria. We have traced this fault farther west than Hoyt (1976). In addition, we have correlated it with a fault labelled "Fault Y," in Yerkes and Lee (1979). The trend we mapped agrees generally with trends published by Zioney et al. (1974), Campbell et al. (1975), Yerkes and Lee (1979), among others, but we have interpreted it as a single continuous trace. It does not offset the seafloor south of Goleta.

Hoyt (1976) mapped the south branch of the Red Mountain between Montecito and Sand Point. We did not find obvious seafloor rupture associated with this fault. The Red Mountain fault is well known as a north dipping high angle reverse fault, up on the north (see Jackson, 1981). It is puzzling that its offshore

extension is very definitely southside-up. Hoyt (1976) has interpreted the north branch as a backthrust off the main north dipping south branch of the Red Mountain. The Red Mountain anticline is mapped by him between these two branches.

The central southside-up fault is mapped as the continuation of the Rincon anticline by Hoyt (1976). We have named the southernmost southside-up fault the "South Rincon fault." Hoyt (1976) also located this fault south of Santa Barbara but does not continue it east as we have shown. The eastern trend of the South Rincon fault is identified by him as a separate fault - the "North fault" - south of Carpinteria and Summerland. In view of our data gap in the center of the South Rincon fault trend, Hoyt's interpretation may be the preferred one.

In the eastern shelf region we found no seafloor expression of the Pitas Point fault zone on four crossings of its trend mapped by Zoney et al. (1974) and Greene et al. (1978). However, the southside-up Oak Ridge fault, a south dipping reverse fault, was easily detected on five crossings (Plate 11, Figure 19). This fault offsets a Pleistocene unconformity and several Pleistocene through Holocene (?) sediment layers above it. It appears to be a growth fault in seismic sections (Figure 19). Also detected beneath the eastern shelf is a now-buried channel cut into the late Pleistocene or Holocene erosion surface (Figure 19, Plate 11). It is most narrow and well-defined in the east and broadens westward. Possibly it is a former distributary of the Santa Clara River. The northern edge of this channel was detected by Hoyt (1976). Contour closure on a Holocene isopach map of Greene et al. (1978) suggests a continuation of the channel east to the Santa Clara River.

V.5 Cojo Bay (offshore LNG site)

Two surveys were done over a 12 sq. n. mi. area of the shelf southeast of the Cojo Bay proposed LNG site (Figure 20). This region was previously surveyed quite extensively by P. J. Fischer and others (Mesa², 1978), using mainly medium penetration sparker and uniboom seismic profiles, plus several lines of side-scan sonar. Our data may provide somewhat more detail on the shallower structures and seabed morphology.

In Plate 12 we show our map interpretation in heavy lines superimposed on the interpretation of Mesa² shown in dotted lines. Our shallower data show general overall agreement with the Mesa² map. Major structures like the Point Conception anticline and the Molino trend are not evident in the high resolution-shallow penetration data. The F1 reverse (north up) fault zone at the edge of the shelf was detected by us as mainly a bathymetric ridge.

A main point of disagreement between the two maps concerns the south branch of the Santa Ynez fault (SBSYF), a left-oblique

slip fault which trends southwest from Sacate. Mesa² (1978) state that no evidence of seafloor breakage could be found associated with this fault trend - implying that the last activity on it was pre-Holocene. Yerkes et al. (1981) note that onshore trenching studies across the fault trace indicate motion of possibly late Pleistocene-early Holocene age. We crossed the offshore trace of the SBSYF about 5 or 6 times and found seafloor breaks closely associated with it but not directly over the trace mapped (deeper) by Mesa² (1978) (Figure 21). Mostly we found northwest side-up separations of one meter or less, or noticeable slope changes. Southeast side-up separations were also noted as might be expected from a strike-slip fault. A review of the original 3.5 kHz records used by Mesa² (1978) established that these seafloor breaks were also evident on their lines which are close to ours. However, their high resolution coverage in this area is somewhat less than ours. Our map interpretation shows these seafloor breaks trending slightly oblique to the SBSYF. It remains to be demonstrated whether these faults are splays from the SBSYF and indicate renewed Holocene movement, or in fact are minor cross faults like others mapped on the shelf, and are not related to it.

VI. SUMMARY AND PROJECT EVALUATION

VI.1 Geological mapping achievements

High quality side-scan sonar data were obtained in sufficient quantity to aid geologic interpretation and mapping in the Anacapa Passage and the Santa Cruz channel. Side-scan data from the Cojo shelf were of moderate quality and not voluminous. Side-scan sonar data from the Santa Barbara-Ventura shelf region were relatively free of prominent features. However, texture analysis could have been done on these data to study variations in sediment distribution. We also obtained a few lines of high quality data from the Santa Rosa-Cortes Ridge (SRA on Figure 1) which show the presence of truncated folds on the ridge. We have not reviewed these data in the text.

We found that side-scan and 3.5 kHz seismic reflection need to be used in parallel if either type of datum is to be correctly interpreted. Depth information (3.5 kHz) is needed to ascertain the dip of bedding seen on side-scan sonar; plan view information (SSS) is needed to determine trends of structures seen on seismic profiles. In the Santa Cruz channel survey, we located an eroded anticline entirely with the side-scan sonar data. This discovery was very important in that it established offset on the Santa Cruz Island fault. The feature could not be seen on the 3.5 kHz reflection system.

Image processing (mosaicking) of side-scan records played a key role in mapping of Anacapa Passage. The complex folding patterns here cannot be mapped track-to-track using only cross section information (3.5 kHz seismics) - trends of folds are

needed. Further, the trends are complex enough that only geometrically corrected side-scan data are useful. The full interplay of the various fold trends was clear only after a digital mosaic was constructed.

Below we summarize the main results of our mapping program for each area:

1. Anacapa Passage

Here the Monterey formation is complexly deformed into east-west trending folds which are cross faulted by NE-SW left offset faults. At the south edge of the Passage (shelf break) we located the Santa Cruz-Dume (or Anacapa-Santa Monica) fault zone. The Monterey formation apparently occupies the entire Passage and abuts the stratigraphically lower Conejo volcanics at the extreme east end of the Passage.

2. Santa Cruz Channel

A truncated NW plunging anticline was found in the NW channel which we correlated with the Christi anticline on SW Santa Cruz Island. This infers about 10 kilometers left offset on the Santa Cruz Island fault since the Miocene. The Santa Rosa Island fault trends NE-SW through the central channel and abuts the Santa Cruz Island fault near that island. This confirms the interpretation of Junger (1976, 1979) based on deep penetration seismic data.

3. Naples shelf and slope

Here six chaotic submarine slides were located on the lower continental slope. Three relatively undeformed slide blocks were found on the upper slope. Origin scars for the mass movement units were found just below the shelf break. The slides are buried to a degree which suggests that they are probably not associated with the 1812 earthquake.

4. Santa Barbara-Ventura shelf

The seabed is dominated by east-west trending structures and especially southside-up faults. One major south-up fault was traced from Goleta to Rincon Point, and corresponds in part to previously mapped portions of the north branch of the Red Mountain fault. This fault displays a maximum of 10 meters offset south of Montecito. Two surveys, in 1979 and 1980, investigated the region south of Santa Barbara. We found no

seafloor disturbance which could be attributed to the August 13, 1978 Santa Barbara earthquake. The Oak Ridge fault may displace the shelf Holocene sediments but we could find no evidence that the Pitas Point fault does so. We found the buried channel of the Santa Clara River off Oxnard.

5. Cojo Bay (offshore LNG site)

Our map here generally agrees with the previous interpretation of Mesa² (1978). In addition we found evidence of seafloor breakage near the trace of the south branch Santa Ynez fault, suggesting that this fault may still be active.

VI.2 Image processing achievements and evaluation

The image processing objectives of this study were achieved in part, but not in full, primarily because of inadequate navigation data. In addition, the sheer bulk of data for A/D conversion and digital processing represents a major barrier for developing a transportable technology for digital pre-processing. Detailed assessments are as follows:

1. At considerable cost in research and computer time, it proved feasible to achieve first-order (approximate) corrections for variable cross and along track scales, to correct to a ground-range display rather than a slant-range display, and to achieve opposite-look (not same-side look) mosaicking.
2. The level of geometric correction achieved with a moderate level of navigation control, and no control over fish dynamics, was insufficient to achieve stereoscopic fusion in the best test set of side-lapping, same-side, stereoscopic imagery we were able to obtain.

As noted by Denbigh (1978) earlier, this disappointing degree of correlation in geometry and particularly in fine structure greatly impedes the visual fusion of images during stereoscopic viewing. Precise navigation control of both vessel and fish, along with same-side, same-height imaging appears essential for achievement of stereoscopy. Fine structure variations will remain as a problem but by analogy with the radar situation for "pepper and salt" images of the type obtained with synthetic-aperture imaging, should not completely deter fusion of separate-track images if precise knowledge of the position, depth and attitude of the fish is available. Probably this level of precision will be best

achieved on an inertially controlled submarine or large fish, suggesting a very large investment for this capability.

3. The ground-range display mosaicking achieved in this project was important for geological interpretation, in confirming the continuity of structures which could not be followed in the near-range on the slant-range paper displays.
4. A wide variety of image enhancement procedures were tested. The most useful were mosaicking of standard deviation images, which proved useful in enhancement of lineations, and contrast stretching along with rectification (Plate 3), which produced a dramatic improvement in image quality and interpretability of sediment patterns and of exposed truncated folds which were at times invisible on the original paper (analog) records; thus the most useful procedures for texture enhancement were relatively simple. More complex enhancements involving sequential median low pass (smoothing) and mean or median high pass (edge-enhancement) filtering produced mixed results in that textural features were suppressed, but lineations were emphasized when followed with the standard deviation filtering and an additional contrast stretch. Inverse (Wiener) filtering, though leading to some improvements in image quality, was not cost-effective (it was the most costly digital enhancement procedure employed) with our data because of the uncertainty in describing the actual system point spread function and the low S/N in the image, as well as the modest gains in image quality from these procedures.
5. Color combination imaging was not attempted because the sufficiently precise navigation control needed for overlaying two images on top of one another was not available.

In summary, the importance of precise navigation data was reconfirmed, as was the need for a continuous record of fish dynamics if the full array of image processing techniques is to be applied to sonar records. A wide variety of special geometric/navigation correction procedures are available in the Fortran language for other users of the same side-scan sonar system. The VICAR software has proven useful for mosaicking, and simple texture and more complex lineation-enhancement procedures (filtered, linear stretch, and standard deviation images) were also shown to be the most useful of those tested. While these are positive

aspects of the study, we are less sanguine that these procedures constitute a broadly applicable technology for surveys of small areas because of the high start-up and familiarization costs involved. For large area surveys we suspect that large systems employed with a stable or inertially navigated platform, and using wide-swath (synthetic aperture) imaging will be more suitable for geologic exploration of the continental shelf.

REFERENCES

Arleth, K. F., 1977. Marine structural geology and geologic evolution south of Santa Rosa and San Miguel islands, California, unpub. M.S. thesis, San Diego State Univ., 161 pp.

Ashley, R. J., R. W. Berry and P. J. Fischer, 1977. Offshore geology and sediment distribution of the El Capitan - Gaviota continental shelf, northern Santa Barbara Channel, California; J. Sedimentary Petrology, 47:199-208.

Belderson, R. H., N. H. Kenyon, A. H. Stride and A. R. Stubbs, 1972. Sonographs of the seafloor. American Elsevier Publishing Co., New York.

Berkson, J. M. and C. S. Clay, 1973. Transformation of sonar records to a linear display. International Hydrographic Review. Contribution No. 292 of the Geophysical and Polar Research Center. Dept. of Geology and Geophysics. University of Wisconsin.

Campbell, R. H., S. C. Wolf, R. E. Hunter, H. C. Wagner, A. Junger and J. G. Vedder, 1975. Geologic maps and sections, Santa Barbara Channel region, California: U.S. Geol. Survey Open File Map 75-123.

Clerici, E., 1977. Über die Anwendbarkeit von Side Scan Sonar zur Erstellung von Topographischen Karten des Meerlsbodens. PHD Dissertation, University of Hanover.

Clerici, E., 1978. Evaluation of relative effectiveness of some image processing techniques applied to side scan sonar data. U.S.-Australia Workshop on Image Processing Techniques for Remote Sensing. Canberra, Australia. May.

Clifford, P., 1979. Real time seafloor mapping. Sea Technology Vol. 20, No. 5. May.

Curran, J. F., K. B. Hall and R. F. Herron, 1971. Geology, oil fields, and future petroleum potential of Santa Barbara Channel area, California: in Cram, I. H., ed. Future Petroleum Provinces of the United States - Their Geology and Potential, AAPG Mem. 15, p. 197-211.

Denbigh, P. N., 1978. Stereoscopic side-scan sonar. Acous.. Letters 2:108-112.

Greene, H. G., S. C. Wolf, and K. G. Blom, 1978. The marine geology of the eastern Santa Barbara Channel with particular emphasis on the ground water basins offshore from the Oxnard Plain, southern California: U.S. Geol. Survey Open File Report 78-305.

Hajic, E. J., 1980. Digital processing of side scan sonar imagery for mapping the Anacapa Passage seafloor in the Santa Barbara Channel: Unpub. M.A. thesis, Univ. California, Santa Barbara, 172 pp.

Hoyt, D. R., 1976. Geology and recent sediment distribution from Santa Barbara to Rincon Point, California: unpub. M.S. thesis, San Diego State Univ., 91 pp.

Ingham, A. E. (ed.), 1975. Sea surveying, Vol. 1: text; vol. 2: illustrations. John Wiley & Sons, New York.

Jackson, P. A., 1981. Structural evolution of the Carpinteria Basin, western Transverse Ranges, California: unpub. M.S. thesis, Oregon State Univ., 107 pp.

Junger, A., 1976. Offshore structure between Santa Cruz and Santa Rosa islands: in Howell, D. G., ed., Aspects of the geologic history of the California Continental Borderland, Pac. Sec. AAPG Misc. Pub. 24, p. 418-425.

Junger, A., 1979. Maps and seismic profiles showing geologic structure of the northern Channel Islands platform, Continental Borderland, California: U.S. Geol. Survey, Misc. Field Studies MFS-991.

Lee, Henry E., 1979. Extension of synthetic aperture radar (SAR) technique to undersea application. IEEE Journal on Ocean Engineering Vol. OE-4, No. 2, April, pp. 60-63.

Luyendyk, B. P., E. J. Hagic and D. S. Simonett, 1978. Image enhancement in side-scan sonar mapping (Abstract), in Proceedings, 12th Internat. Symp. on Remote Sensing of Environment, Manila, Philippines, April 20-26, 1978, p. 119.

Mesa² Inc., 1978. A geophysical and geologic evaluation of the offshore extension of the Santa Ynez fault, South Branch, Dept. Geosciences, Cal. State Univ., Northridge (rept. for Dames and Moore, Inc., Los Angeles), 19 pp.

Mudie, J., W. Normark, E. Cray, 1970. Direct mapping of the seafloor using side-scanning sonar and transponder navigation. Geol. Soc. Am. Bull., 81:1547-1554.

Narendra, P. M., 1981. A separable median filter for image noise smoothing. IEEE Transactions on Pattern Analysis and Machine Intelligence, Vol. PAMI-3, No. 1. January, pp. 20-29.

NTIS, 1977. Weekly Government Abstracts, June.

Pace, Nicholas G. and Catherine M. Dyer, 1979. Machine classification of sedimentary sea bottoms. IEEE Transactions on Geoscience Electronics, Vol. GE-17, No. 3, pp. 52-56.

Paluzzi, P., 1976. Analysis of imagery for marine resource exploration. Proceedings Caltech/JPL Conference on Image Processing Technology, Data Sources and Software for Commercial and Scientific Applications, California Institute of Technology, JPL SP 43-40, Pasadena, November 3-5, p. 12-1 to 12-9.

Paluzzi, P., W. Normark, G. Hess, H. Hess and M. Cruckshank, 1976. Computer image processing in marine resource exploration. Proceedings for Joint IEEE-MTS Oceans '76 Conference, Washington, D.C., September 13-15, 4D-1 to 4D-10.

Prior, David B., James M. Coleman and Louis E. Garrison, 1979. Digitally acquired undistorted side-scan sonar images of submarine landslides, Mississippi River delta. *Geology* 7:423-425.

Sanders, J. E., K. O. Emery and E. Uchupi, 1969. Microphotography of five small areas of the continental shelf by side-scanning sonar. *Geol. Soc. Am. Bull.* 80:561-572.

Standard Oil Co. of California, 1976. Report to California State Lands Commission for FEIR on resumption of drilling. August.

Spiess, F. N., C. D. Lowenstein, D. E. Boegeman and J. D. Mudie, 1975. High resolution sonars deep in the ocean. *U.S. Navy Journal of Underwater Acoustics*. Vol. 25, No. 1. Jan.

Soutar, A. and P. A. Crill, 1977. Sedimentation and climatic patterns in the Santa Barbara Basin during the 19th and 20th centuries. *Geol. Soc. Amer. Bull.* 88:1161-1172.

Sutton, J. L., 1979. Underwater acoustic imaging. *Proc. IEEE* Vol. 67 No. 4 April, pp. 554-566.

USGS, 1975. Oil and gas development in the Santa Barbara Channel outer continental shelf off California. Draft Environmental Statement DES 75-35, 3 vols, Prepared by U.S. Geological Survey.

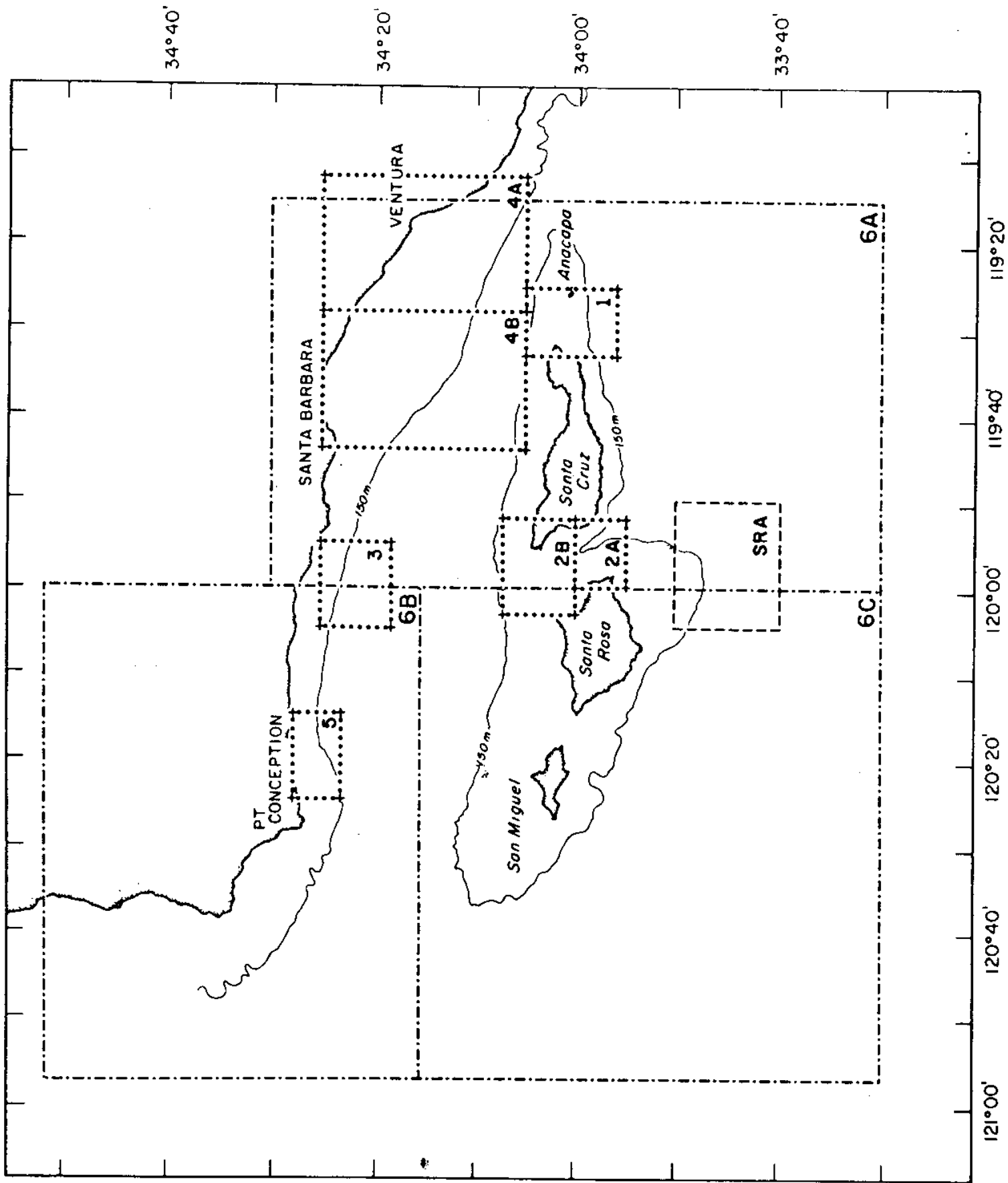
Vedder, J. G., L. A. Beyer, A. Junger, G. W. Moore, A. E. Roberts, J. C. Taylor and H. C. Wagner, 1974. Preliminary report on the geology of the continental borderland of southern California. U.S. Geological Survey Misc. Field Studies Maps MF-624, 34 p., 9 sheets.

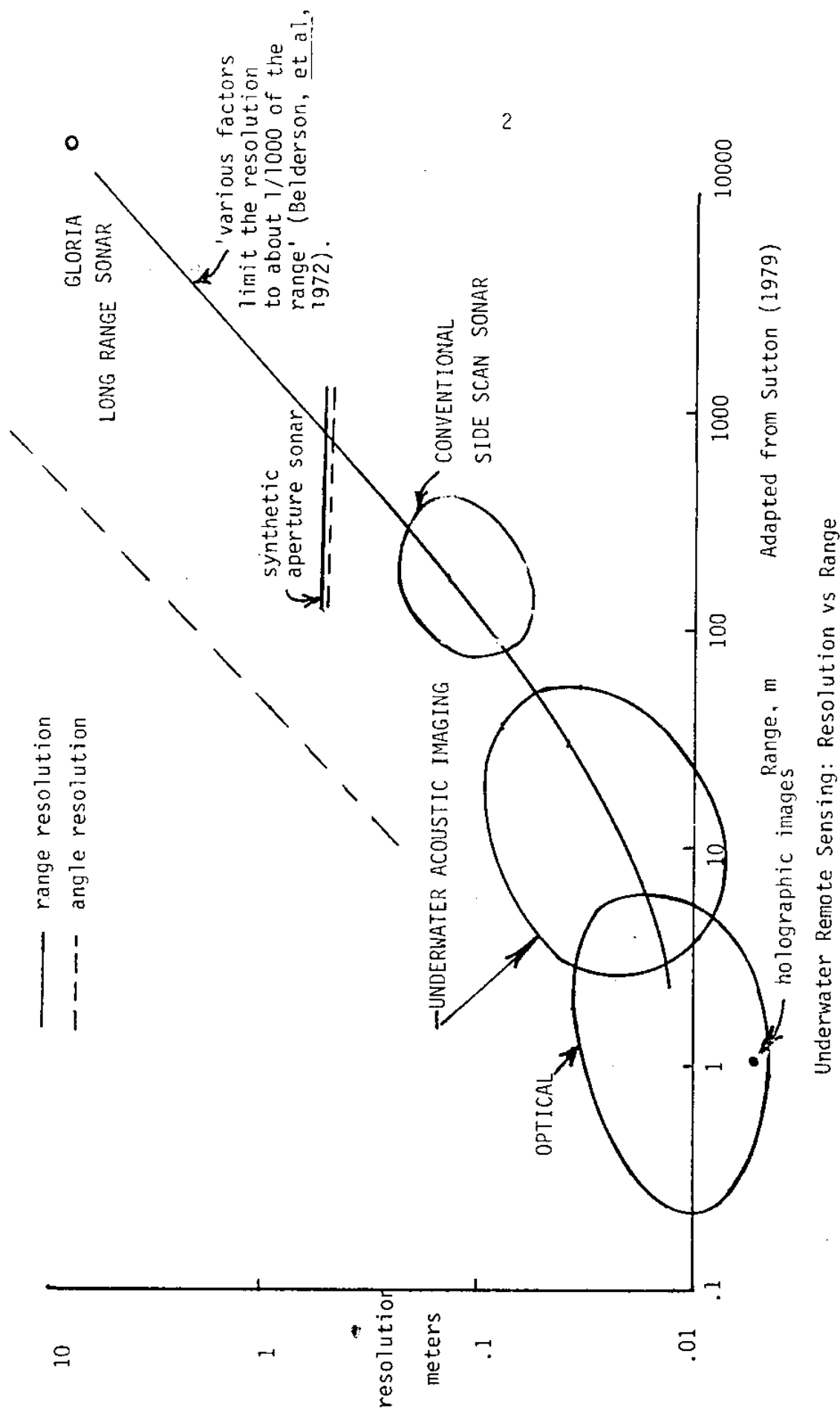
Walker, C. D. T, 1978. Development of a ground speed corrected side-scan sonar display system. *Ultrasonics*, May, pp. 108-110.

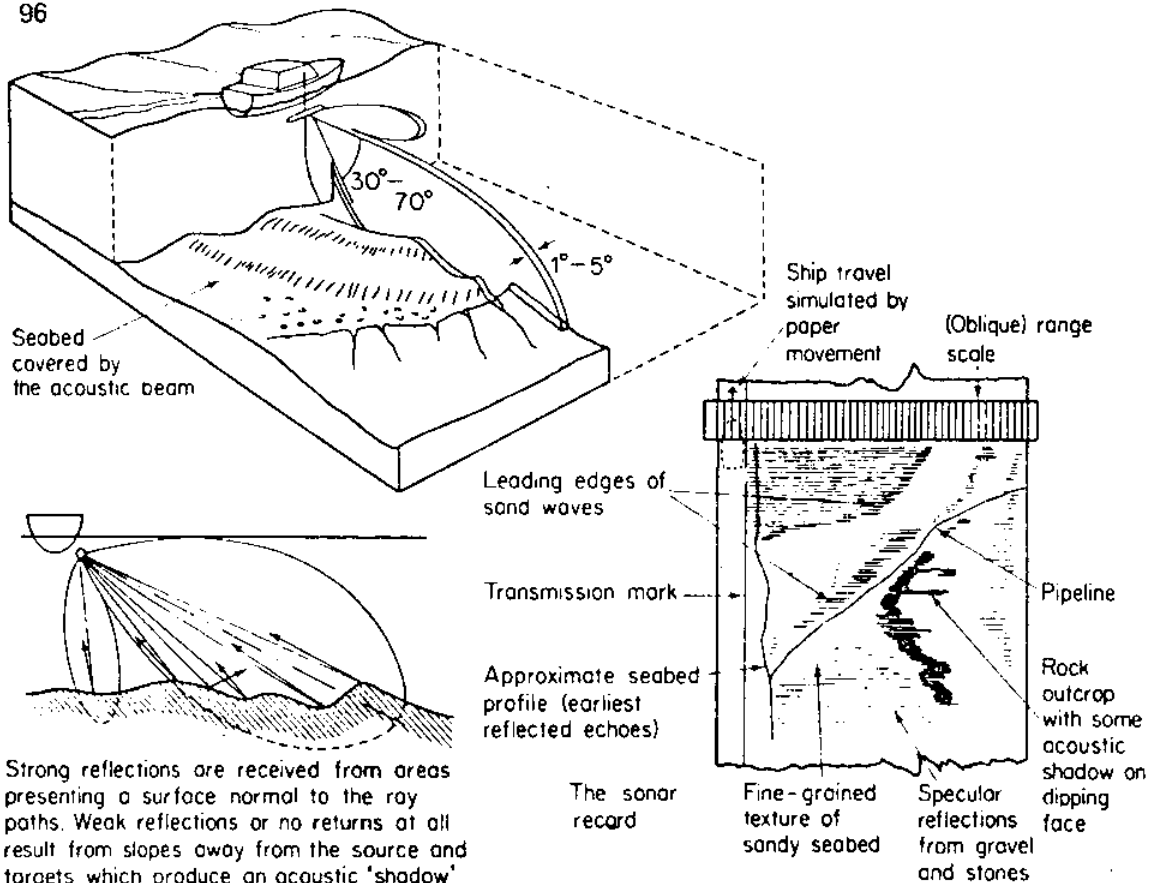
Weaver, D. W., D. P. Doerner and B. Nolf, 1969. Geology of the northern Channel Islands. AAPG-SEPM Special Publ., 199 pp.

Yerkes, R. F., A. G. Greene, J. C. Tinsely and K. R. Lajoie, 1981. Seismotectonic setting of the Santa Barbara Channel area, southern California. U.S. Geol. Survey, MF-1169 (with text).

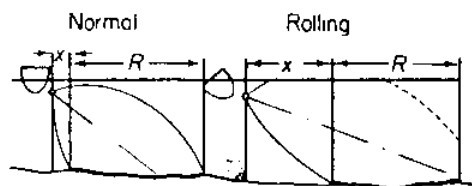
Ziony, J. I., C. M. Wentworth, J. M. Buchanan-Banks and H. C. Wagner, 1974. Preliminary map showing recovery of faulting in coastal southern California. U.S. Geological Survey Misc. Geol. Inv. Map. 585.



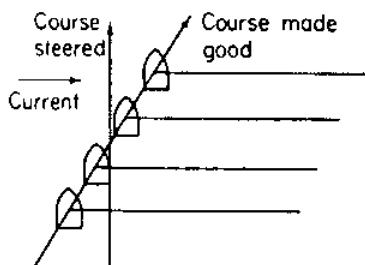




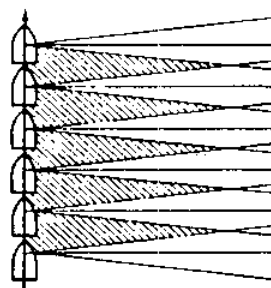
The side-scan mode of operation.



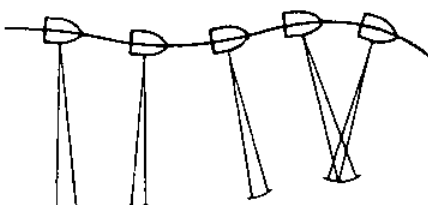
The effect of roll on the seabed 'lane' coverage



Slant horizontal coverage due to current drift

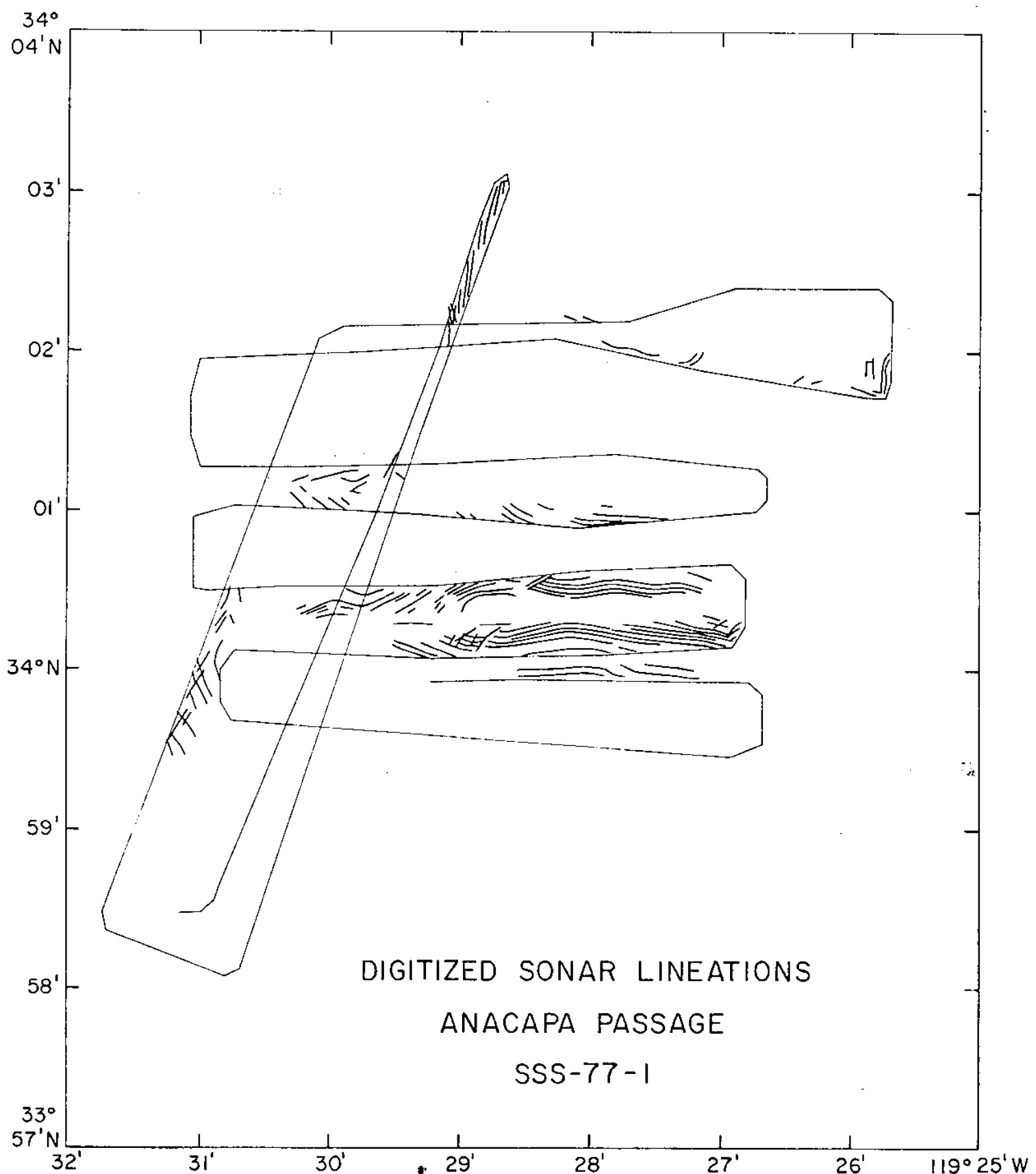


Gaps in coverage due to beam width, pulse repetition rate and ship's forward speed

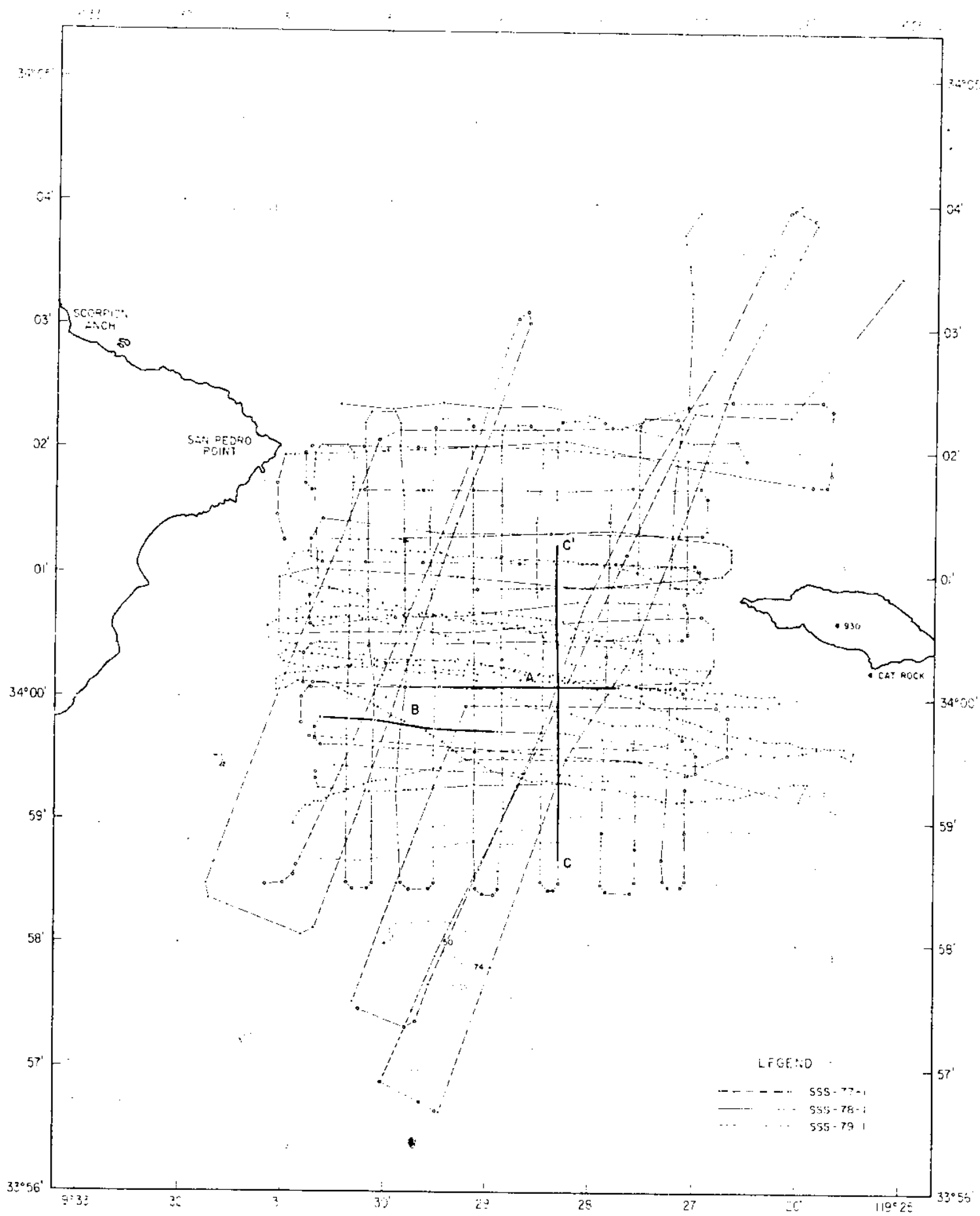


Gaps and overlaps due to yaw

The factors affecting side-scan coverage and resolution.



ANACAPA PASSAGE



SECTION "B"

Dips are to north

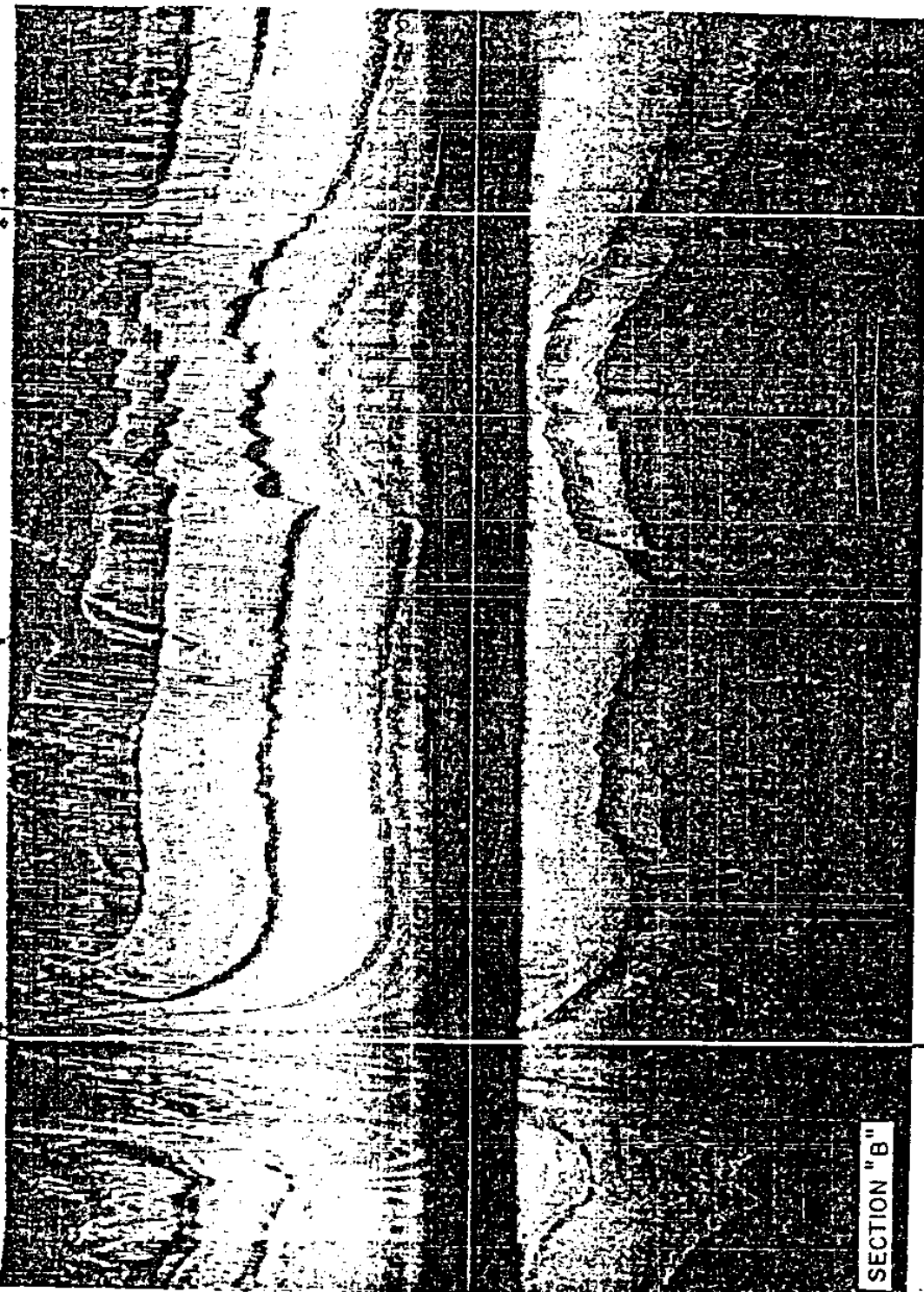
400
meters

WEST

NORTH

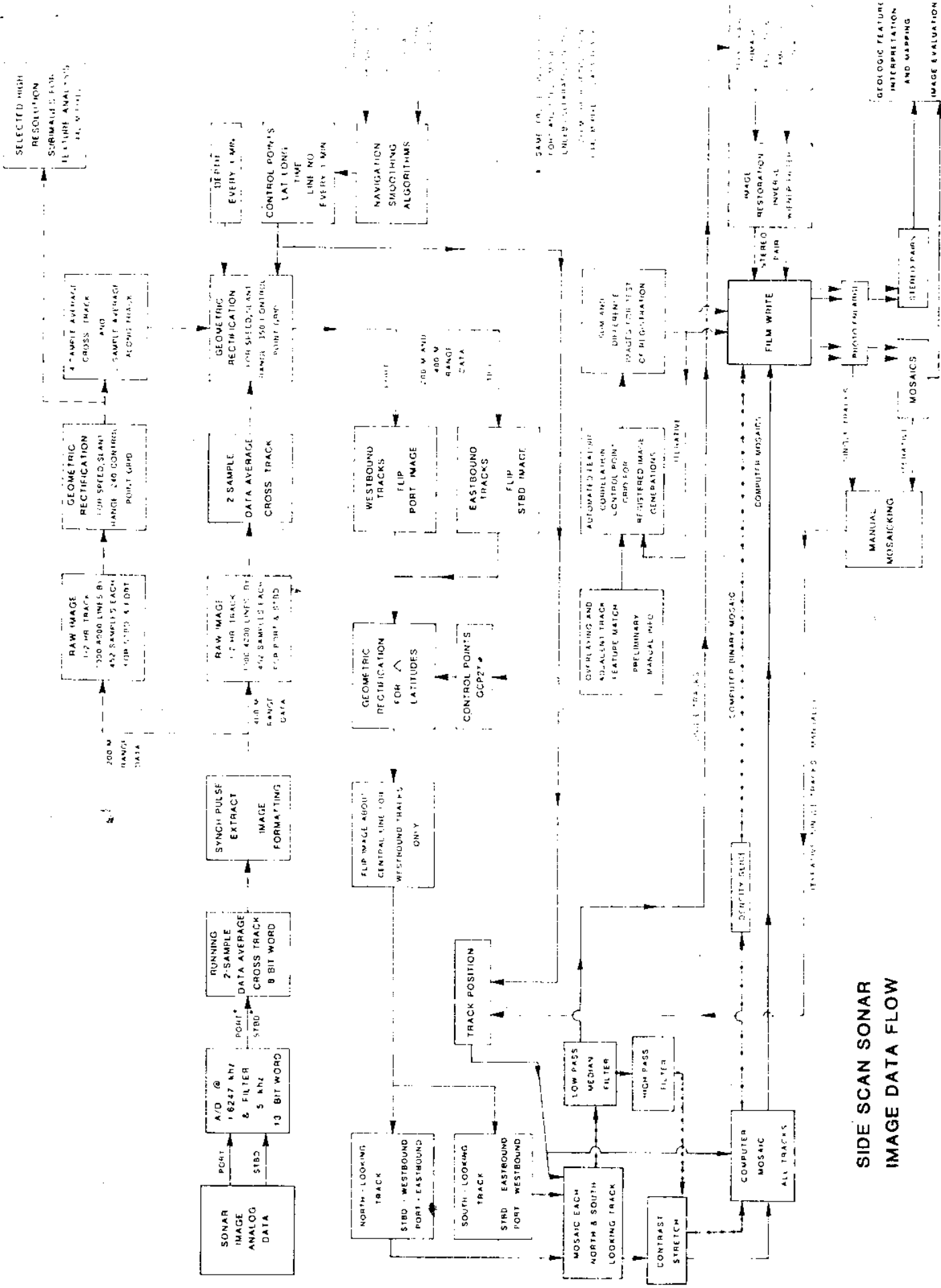
EAST

SOUTH



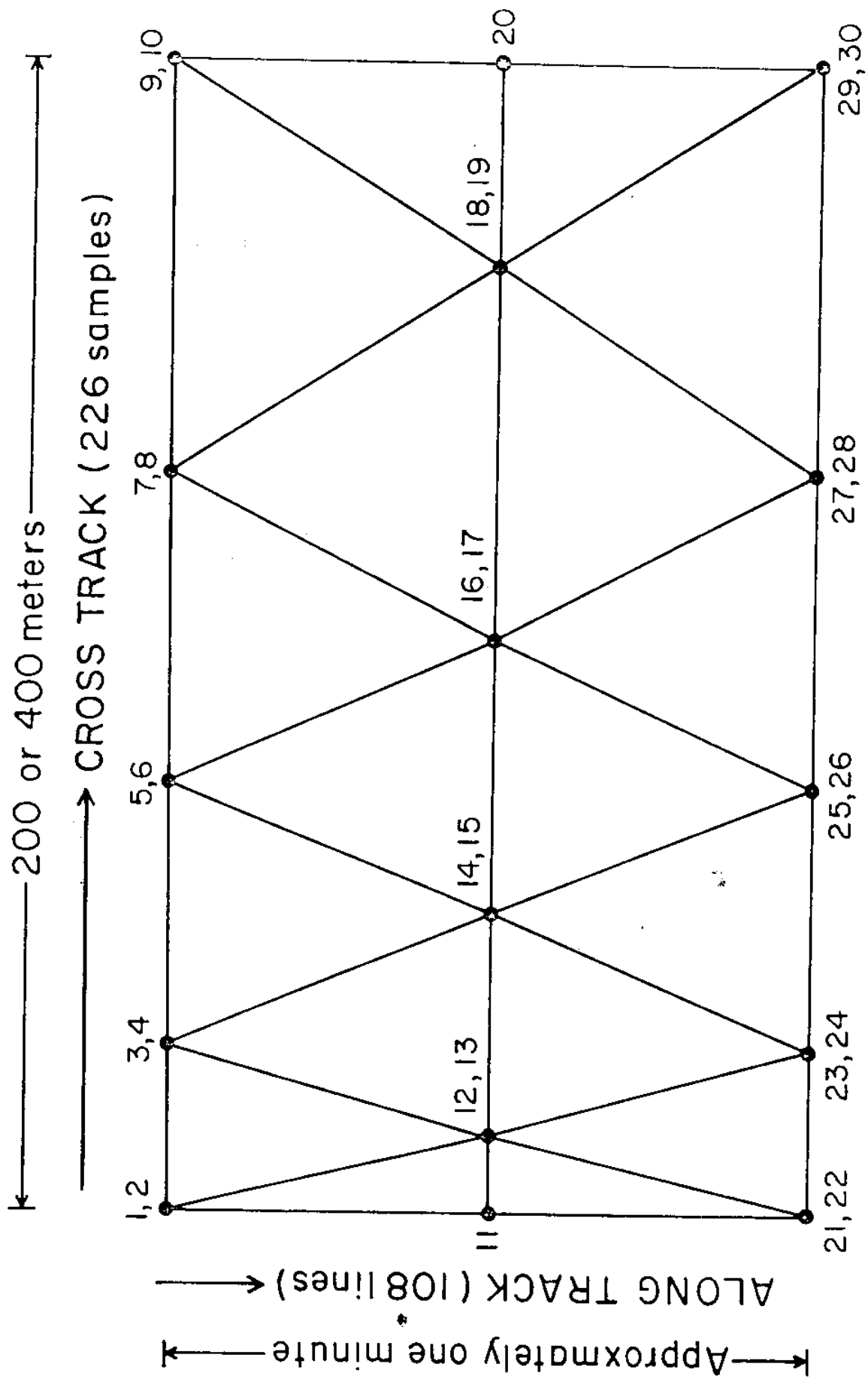
SECTION "B"

2.66 kilometers

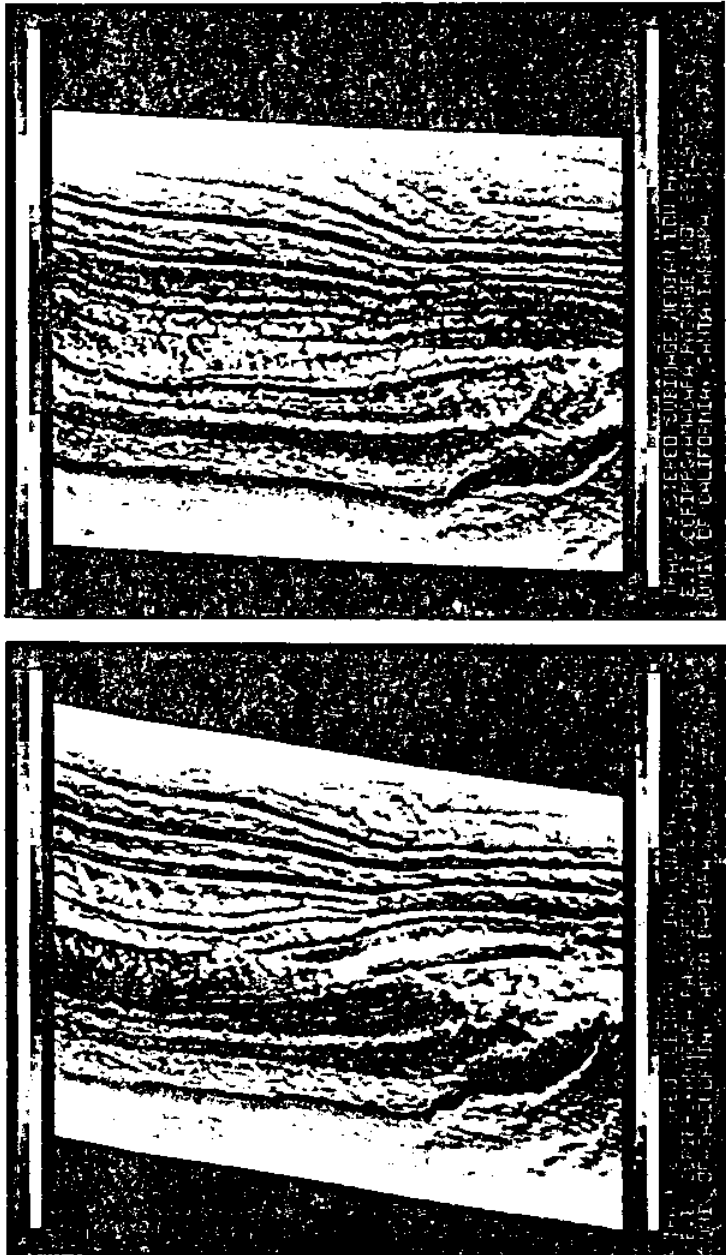


SIDE SCAN SONAR IMAGE DATA FLOW

GEOMETRIC RECTIFICATION GRID



400 m

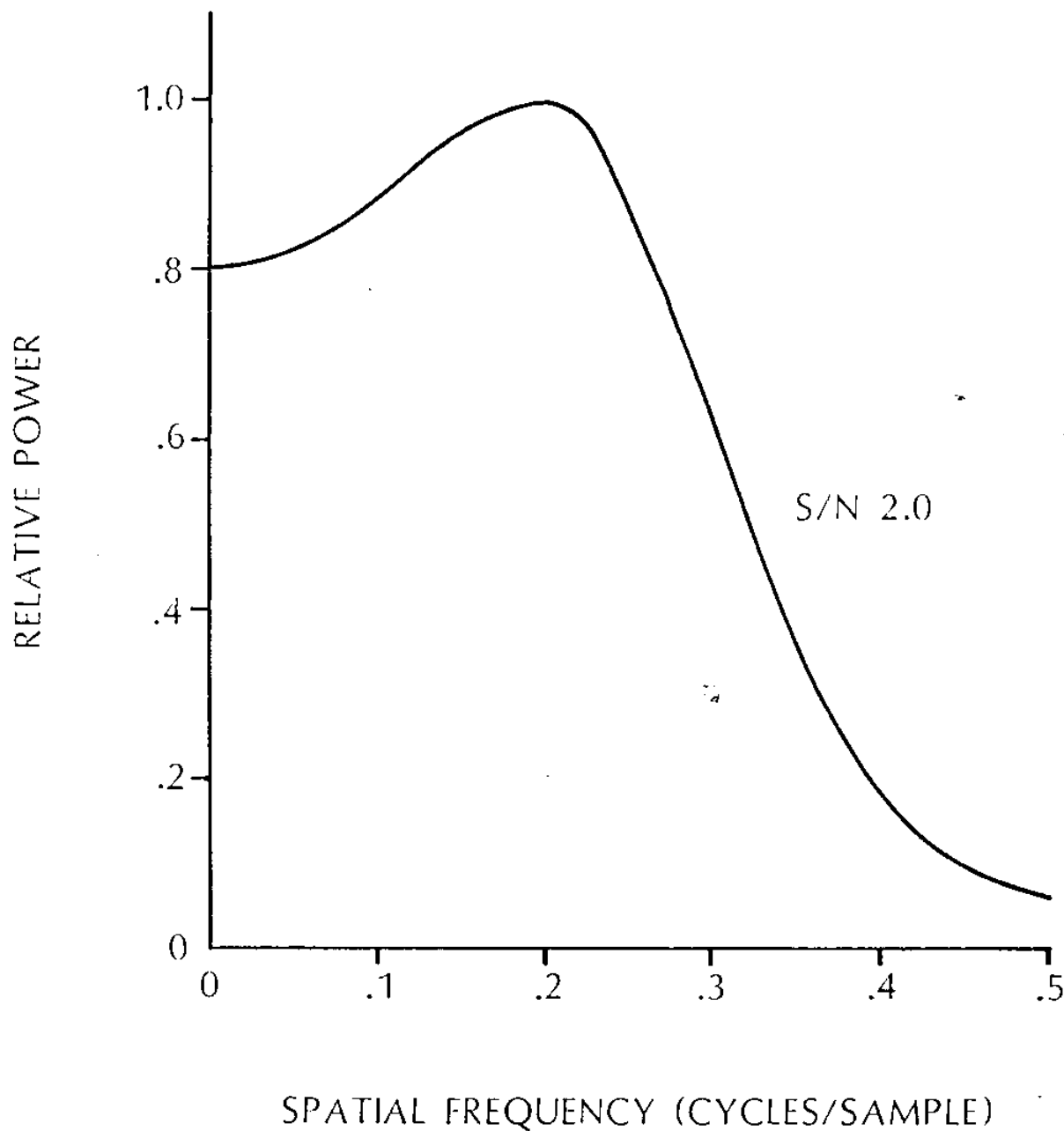


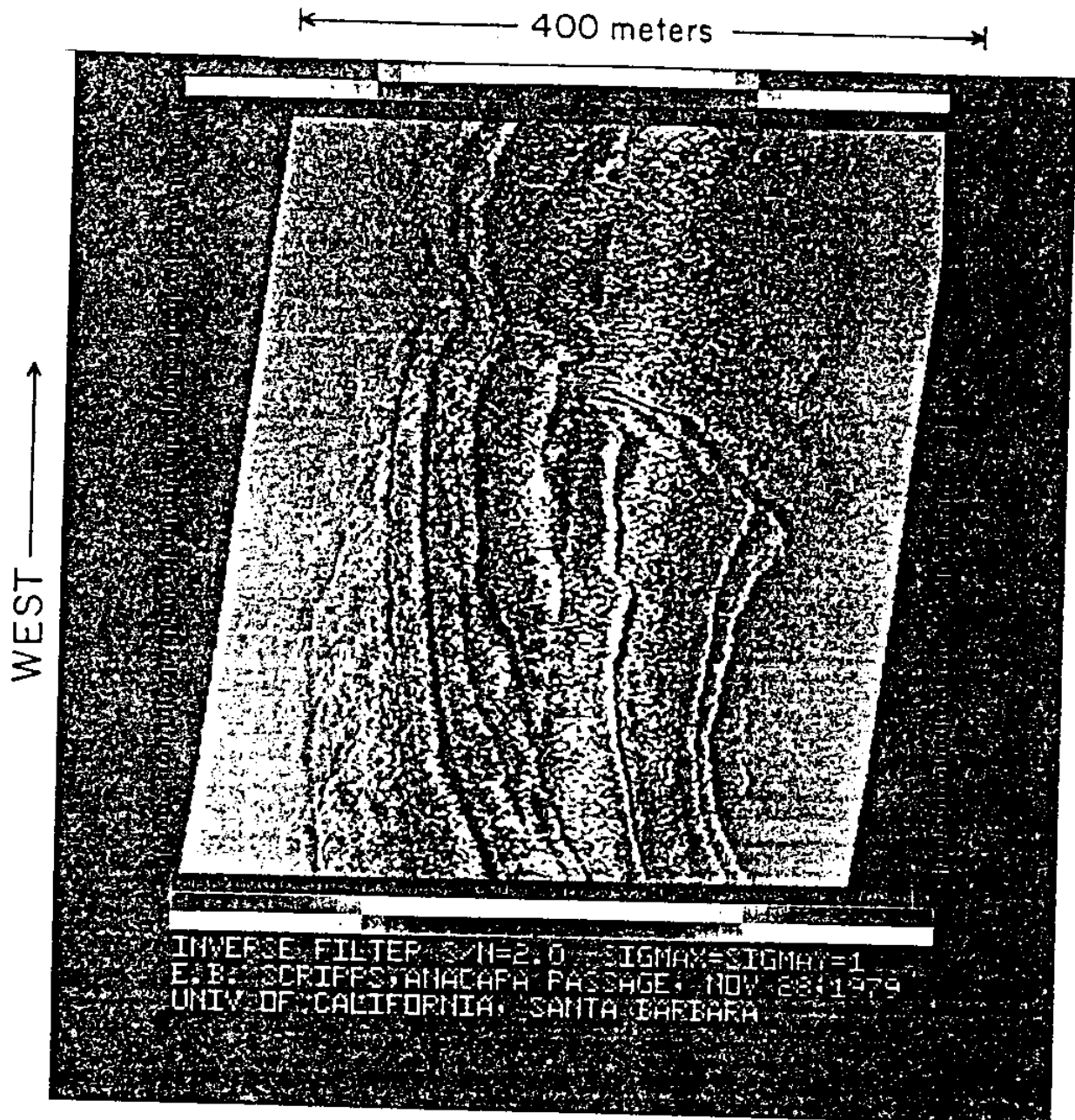
← WEST

Vicinity 34°N , $119^{\circ}27' \text{W}$

Anacapa Passage

INVERSE FILTER TRANSFER FUNCTION

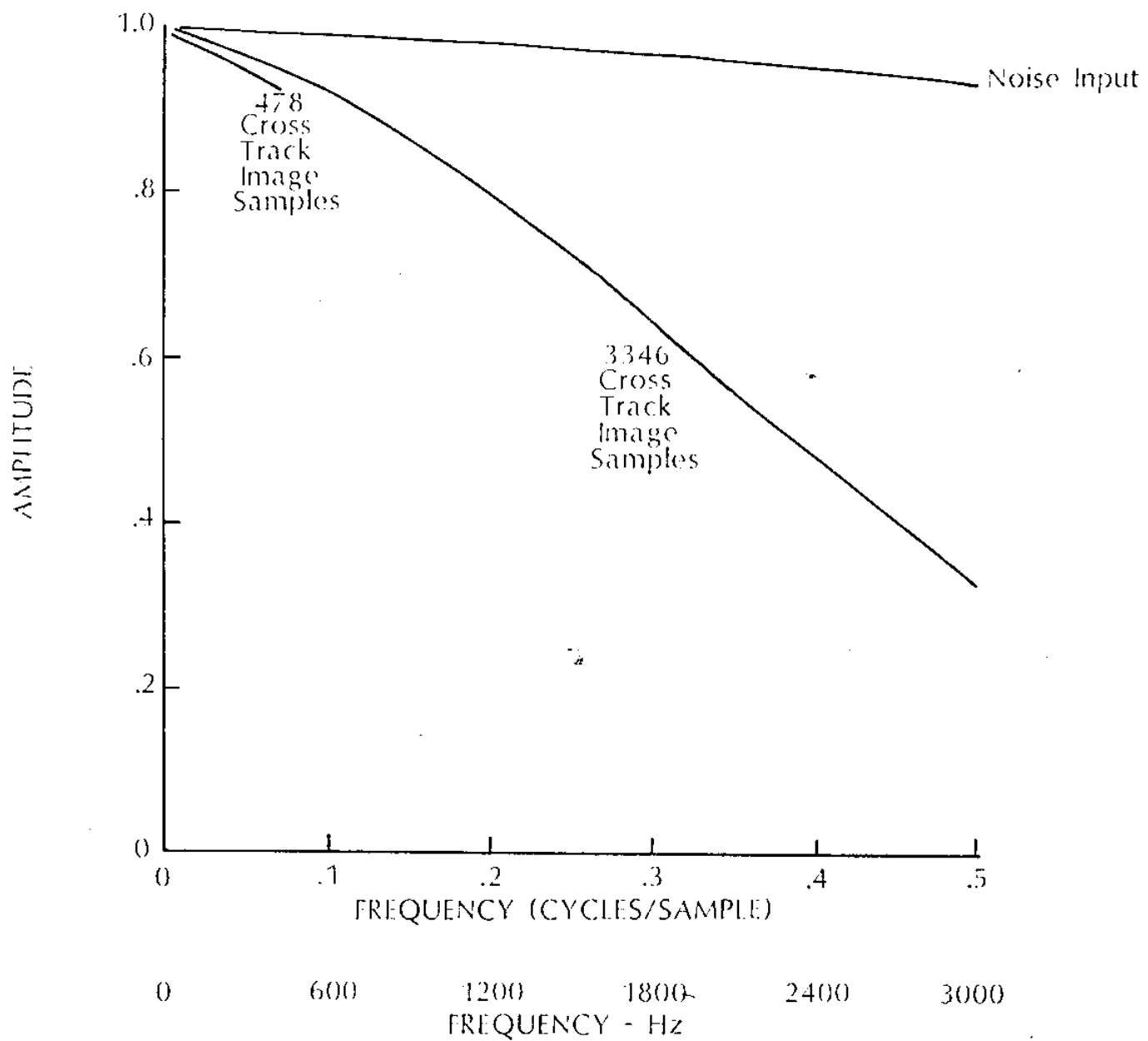


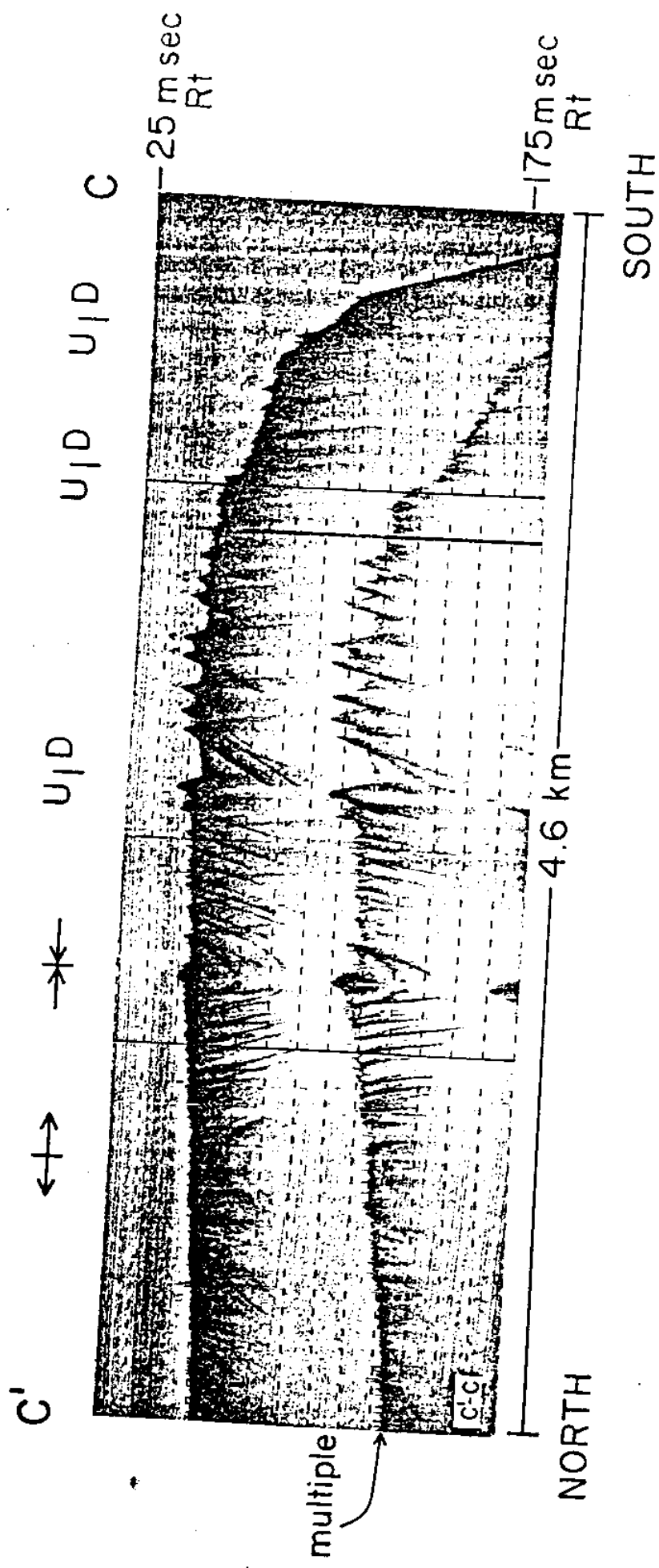


NORTH →

Vicinity 34.3° N, $119^{\circ} 29'$ W
Anacapa Passage

SYSTEM MODULATION TRANSFER FUNCTION DETERMINED
FROM LEADING EDGE OF SYNCH PULSE





ANACAPPA PASSAGE

SECTION "A"
NEAR 34°00' N



EAST

→ NORTH

WEST

syncline
axis

SECTION "A"

2.7 kilometers

10

18.3 meter

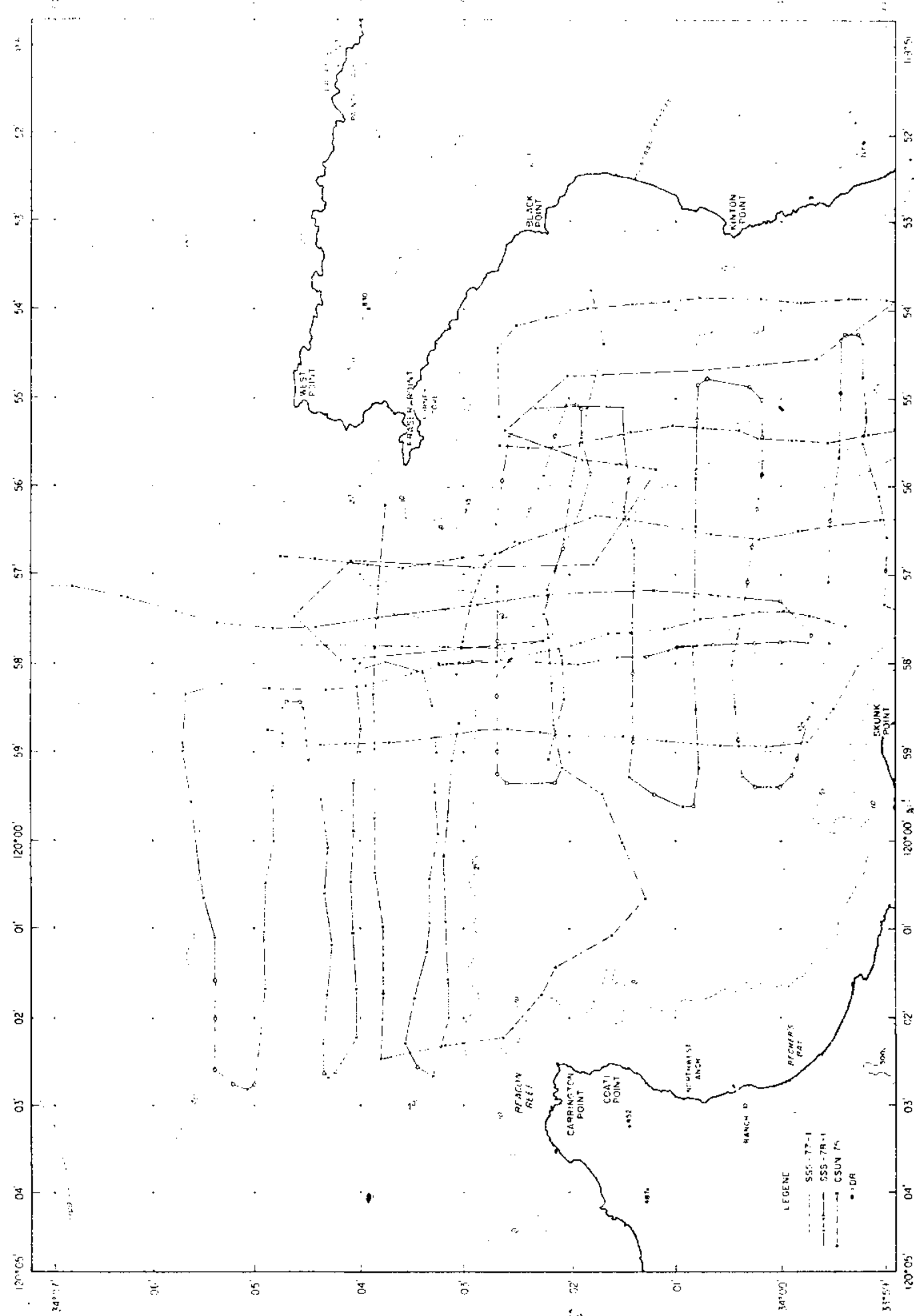
WEST

— — — — —
SECTION "A"

True dips to north

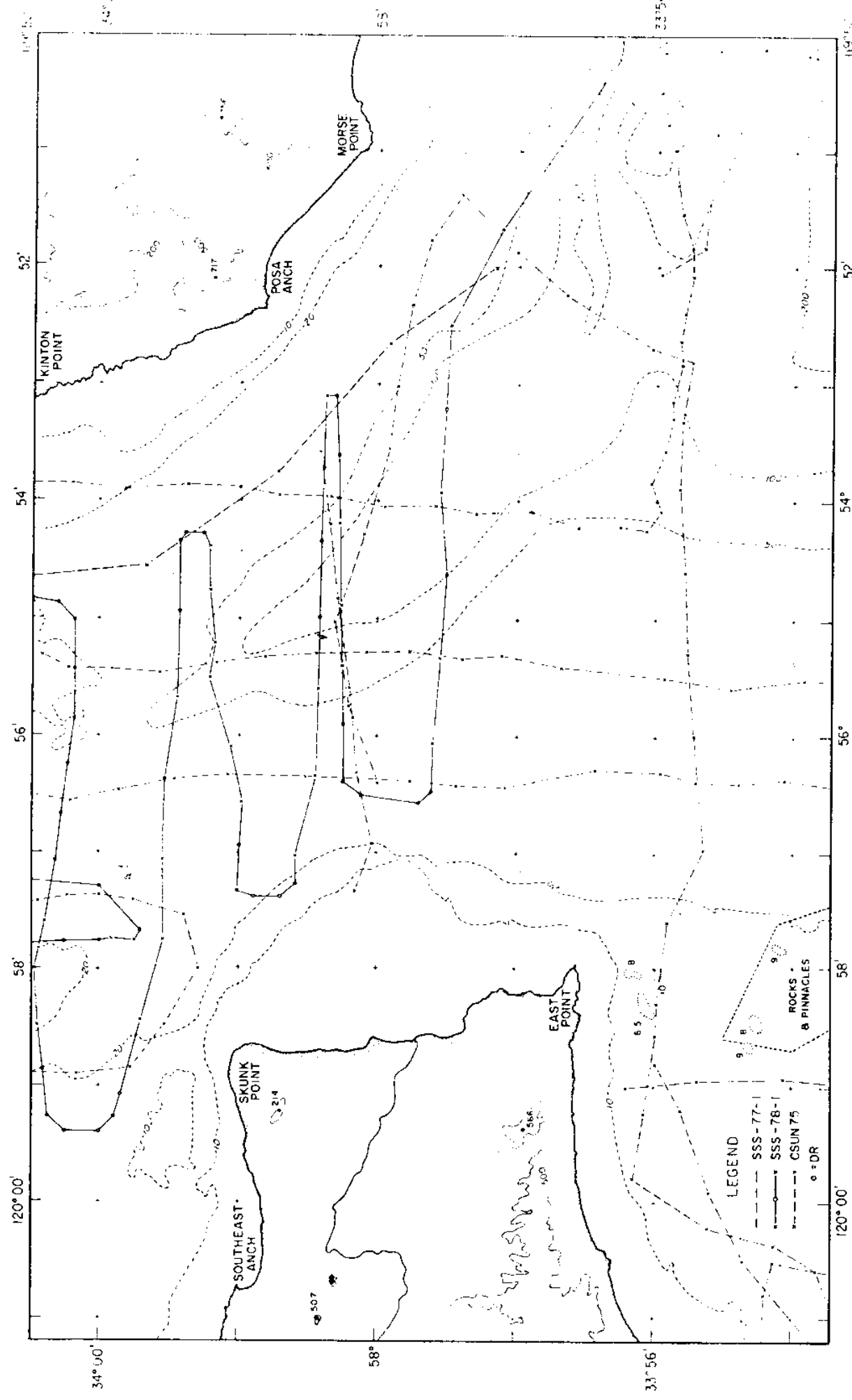
TIA

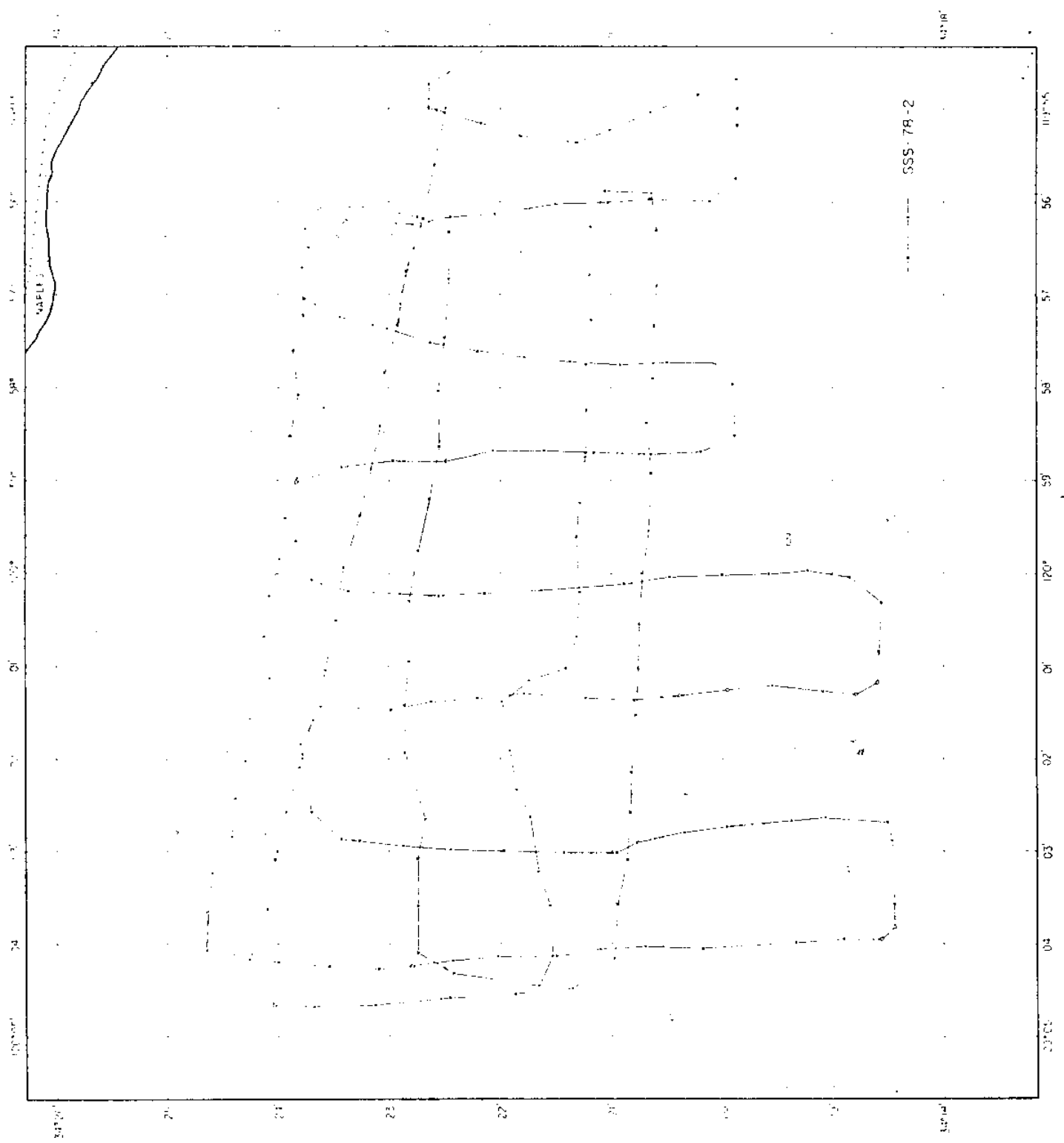
SANTA CRUZ CHANNEL

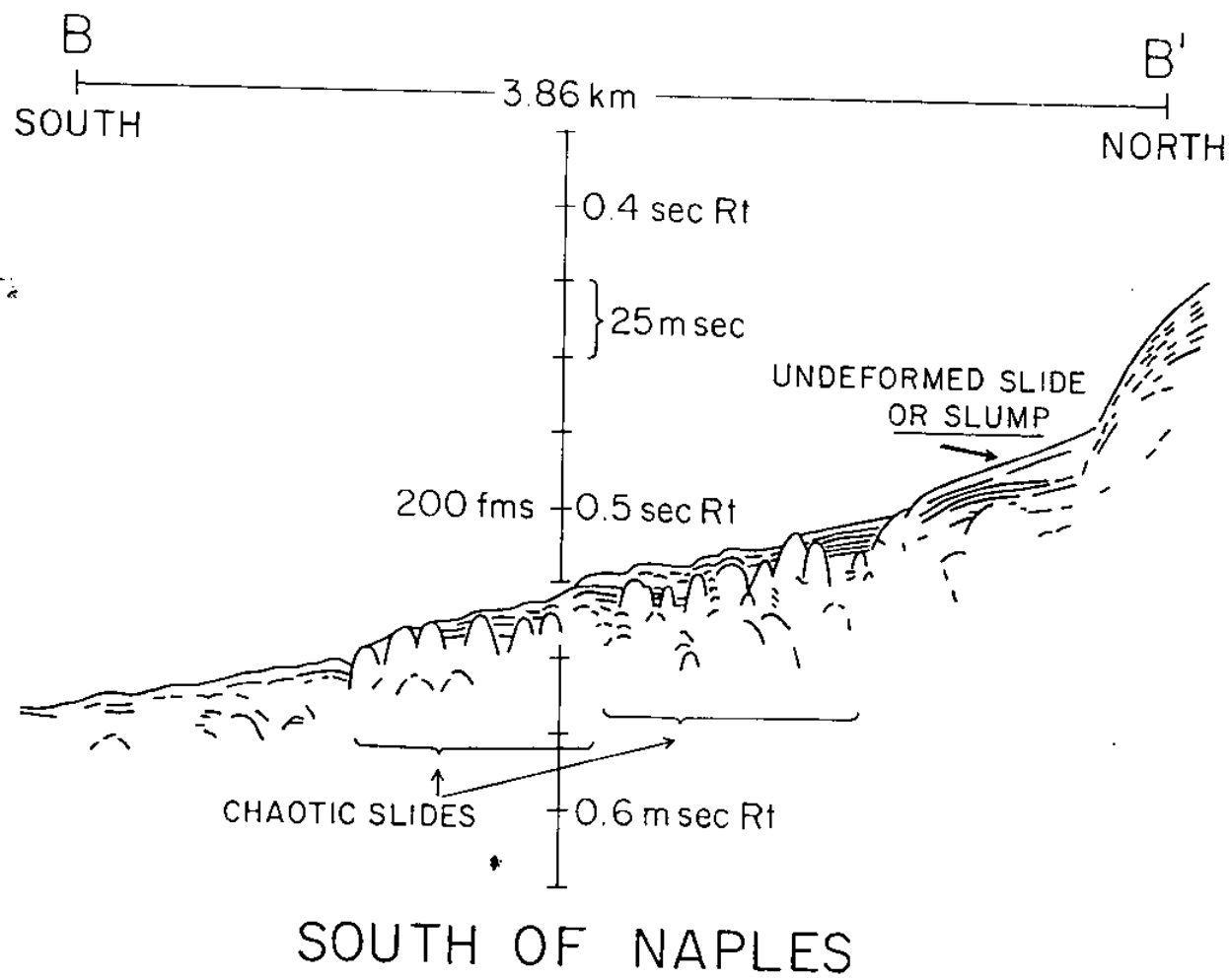
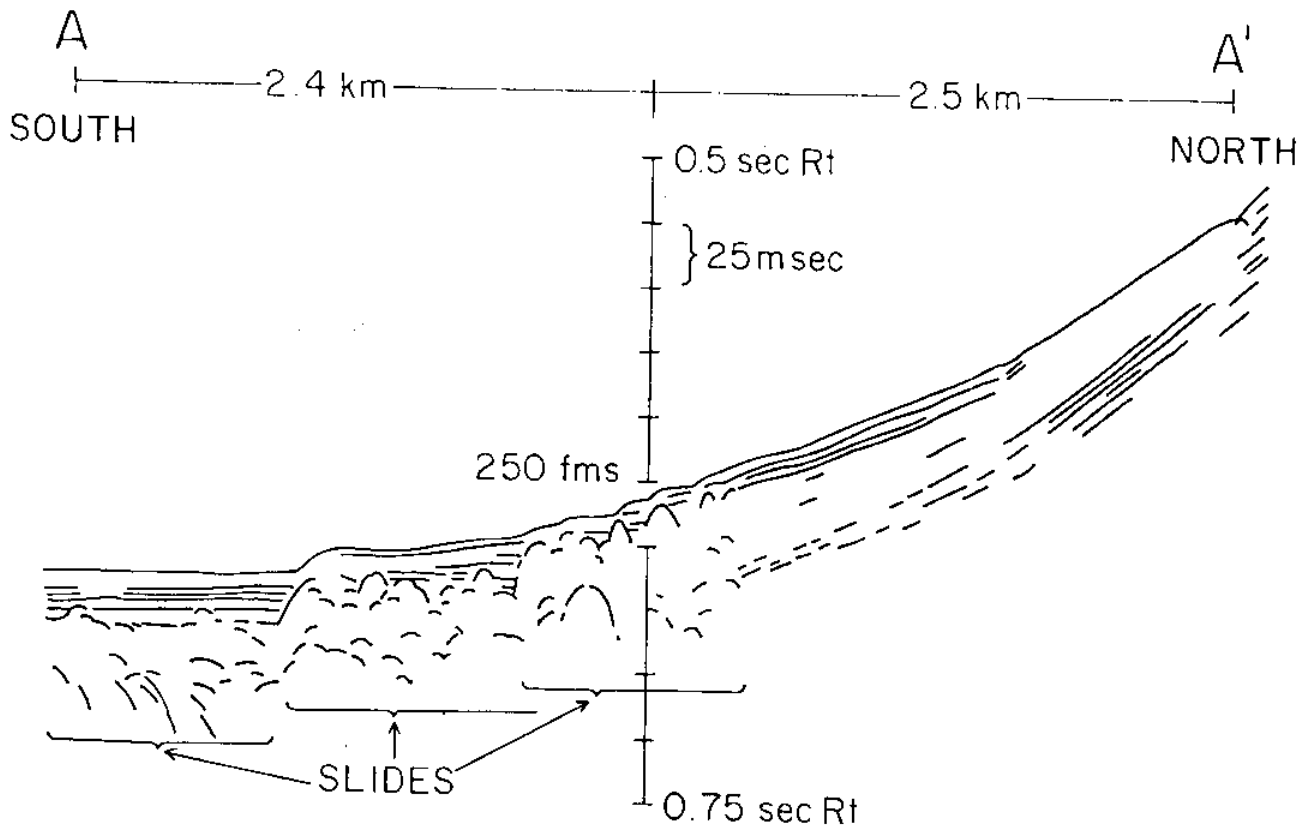


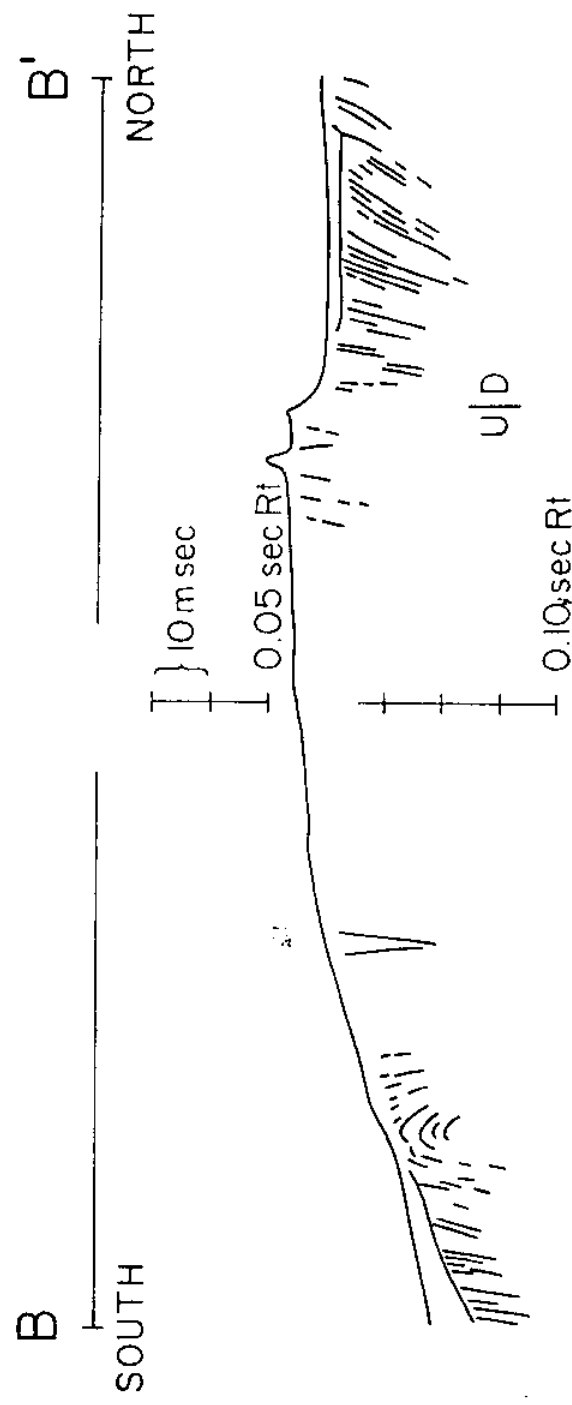
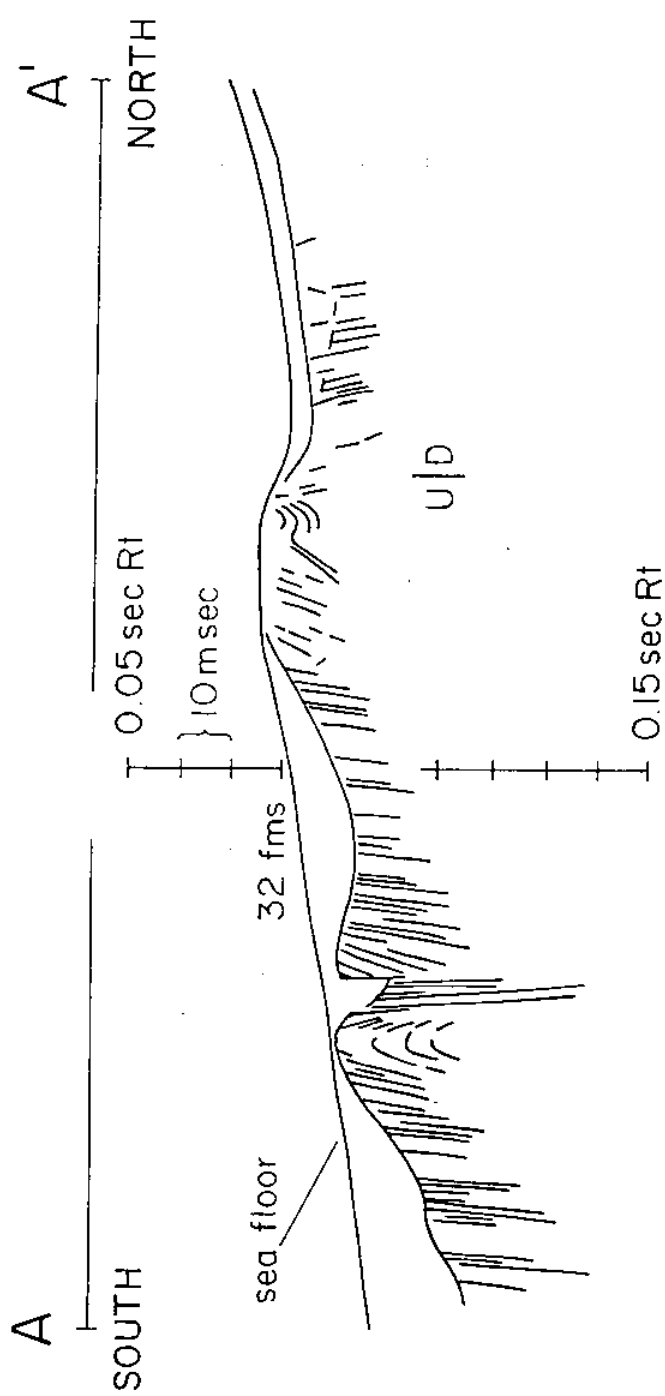
SANTA CRUZ CHANNEL

2 A

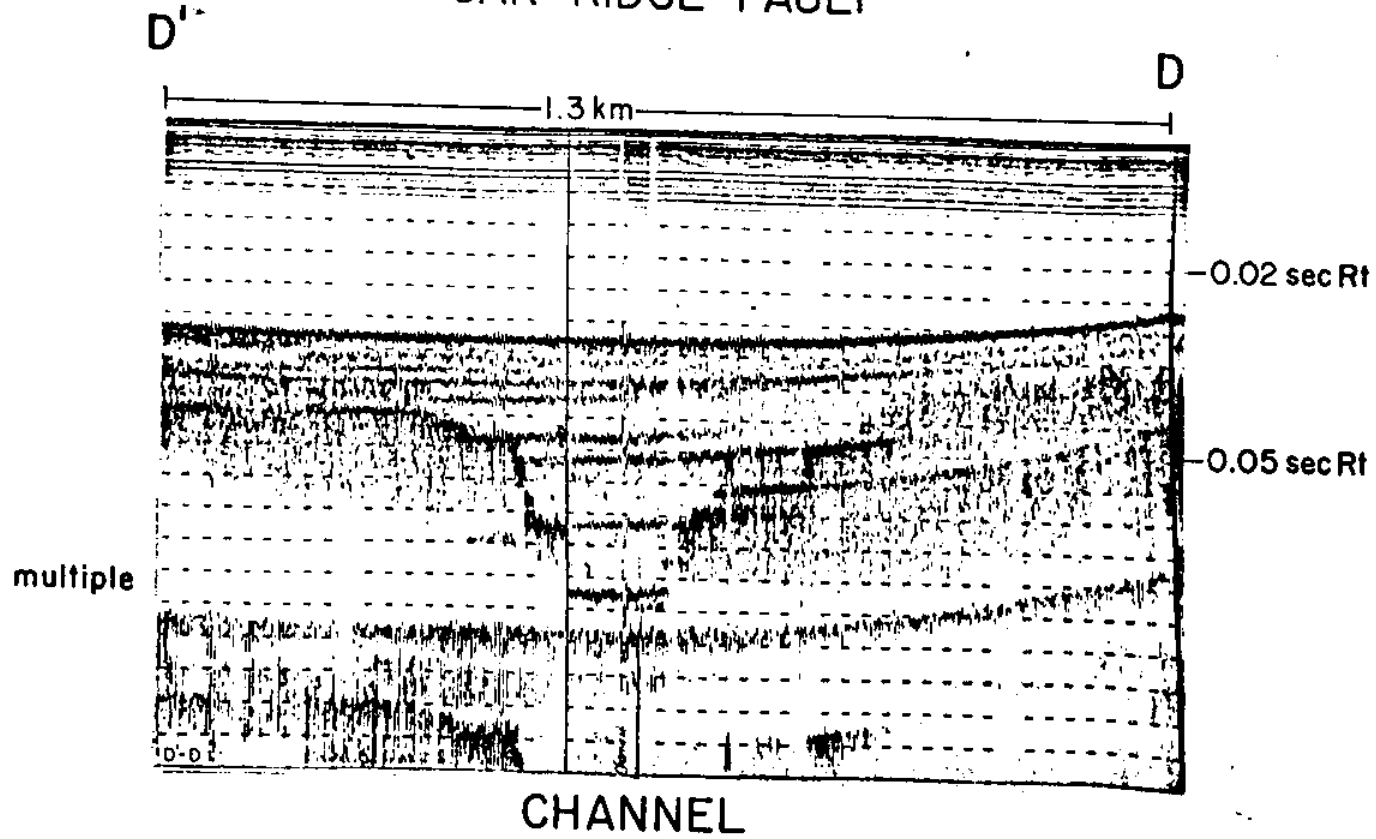
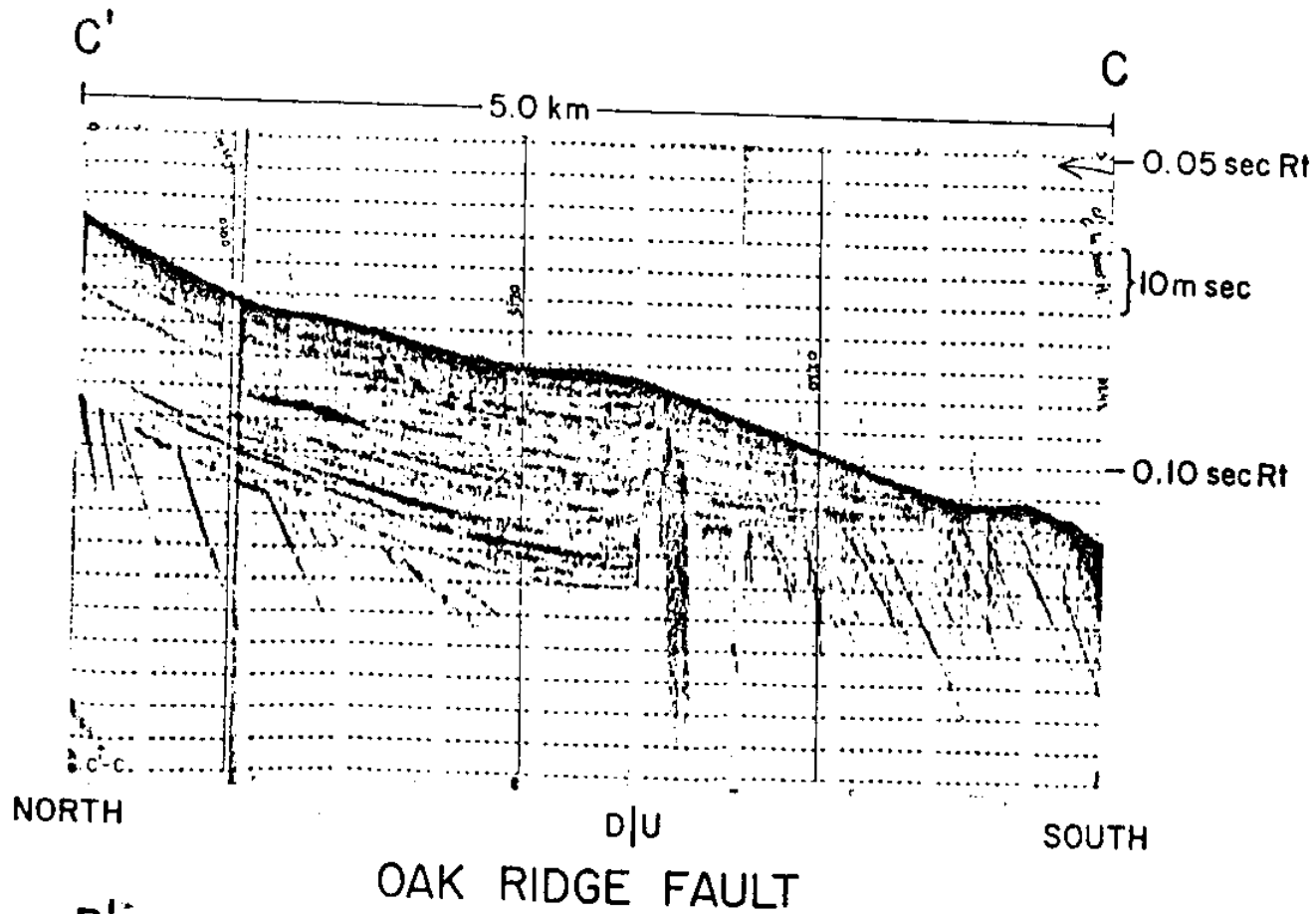


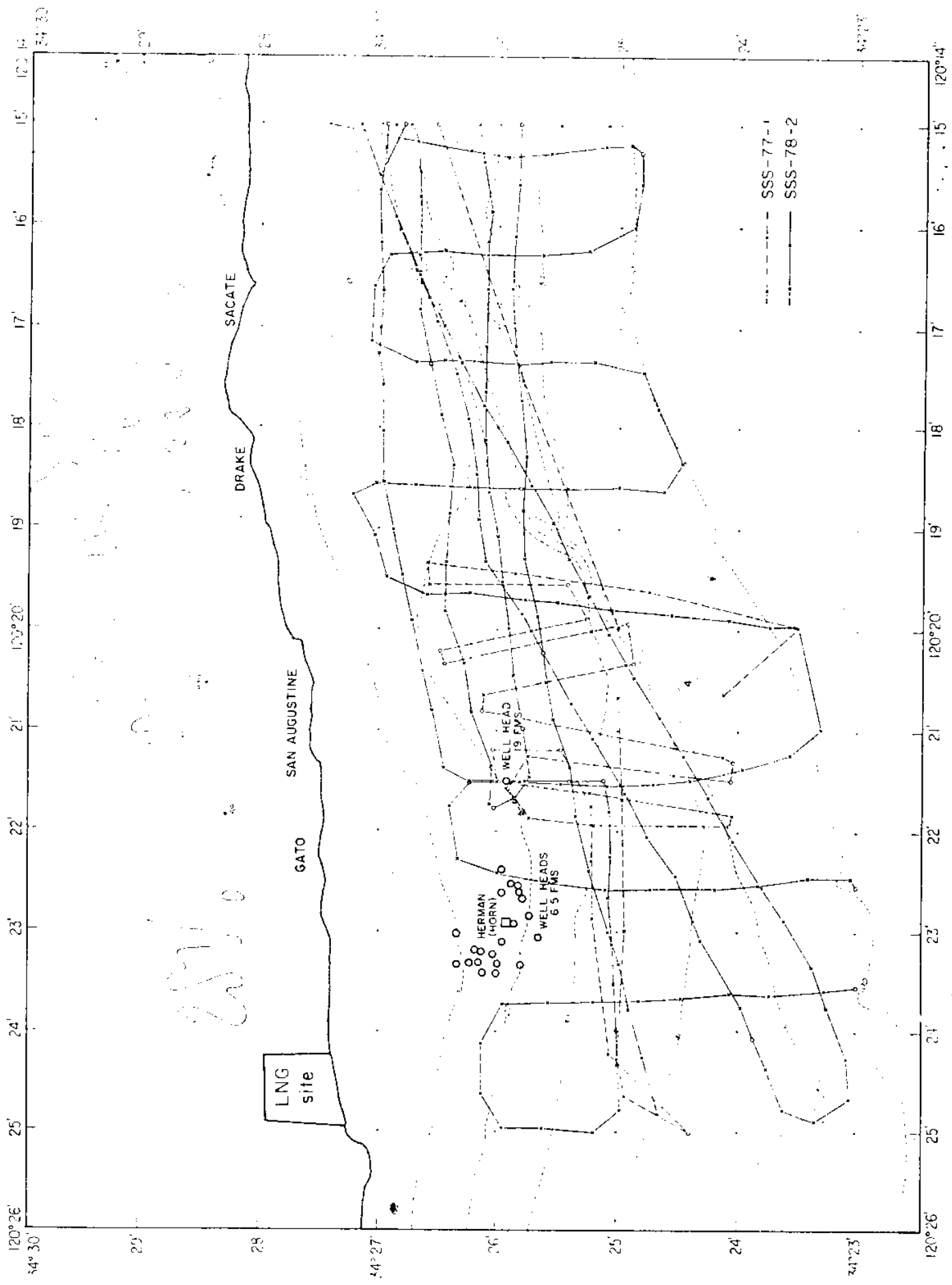


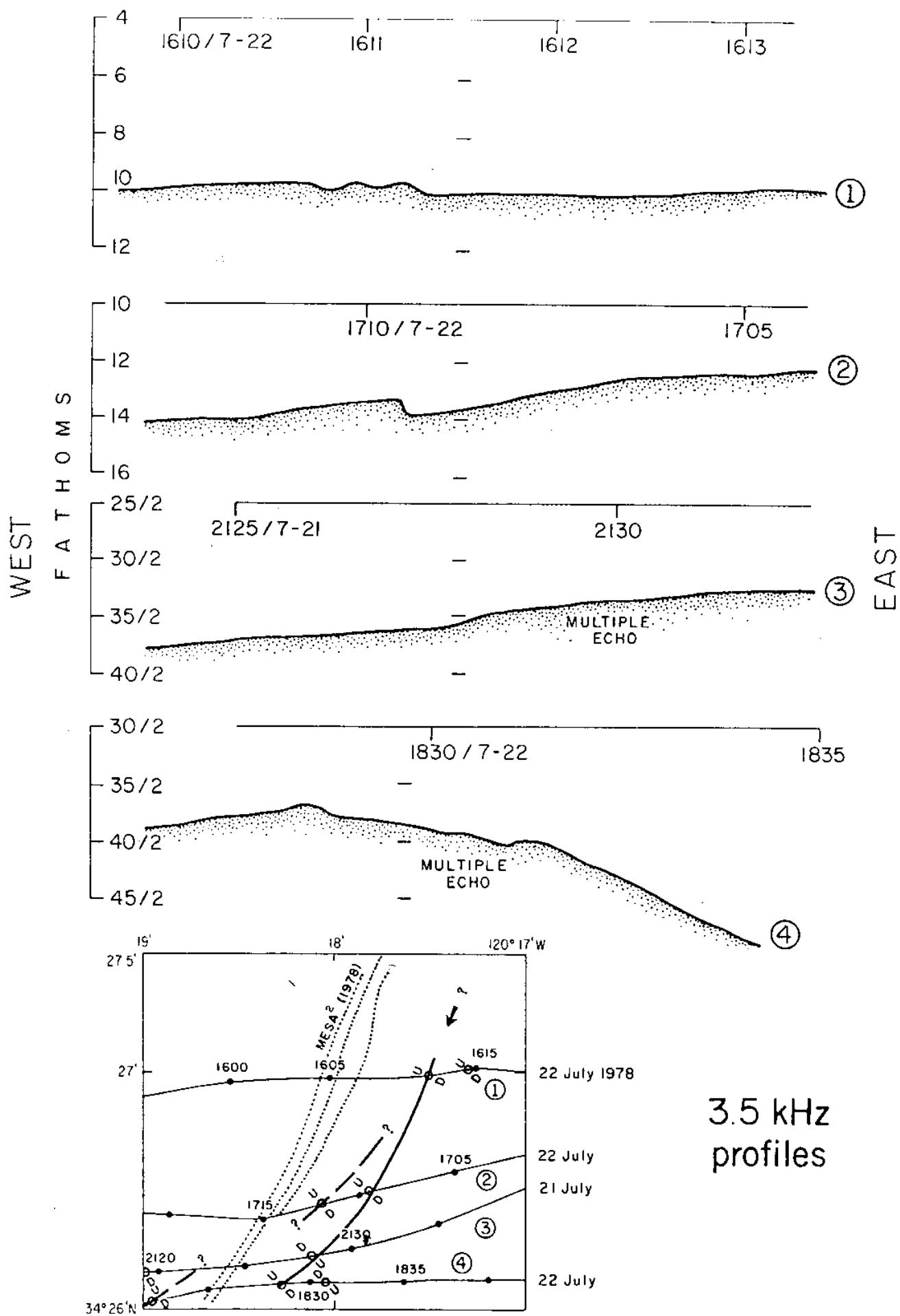




SOUTH OF SANTA BARBARA







APPENDIX 1

Digital acquisition and processing of LORAN-C navigation: Summary and explanation of the navigation programs

by

David Naar

A.1.1 Overview

This documentation explains how to filter and modify the LORAN navigation data from the side-scan cruises. The data consist of precise LORAN fixes and accurate RADAR fixes. At sea, the "NAVLOG" program simultaneously writes LORAN fixes on paper and disc three times a minute (Figures A.1.1 and A.1.2). RADAR fixes are usually taken every 15 minutes by the ship's navigator. A handwritten navigation log is also kept of RADAR fixes, LORAN fixes, ship speed, and ship course.

Our digital navigation scheme has progressed in two steps. First, we designed hardware and software to write 23 second-interval LORAN fixes to a computer disc. These data were then processed onshore according to the flow in Figure A.1.2. A second effort was to automate the onshore scheme to produce real-time unedited navigation track plots during the survey. This processing flow is shown in Figure A.1.1. The real-time flow uses essentially the same software as the onshore processing. At present, we still have a few development changes to make on the real-time package. A final test at sea will take place in September 1981.

The first part of the digital processing is to write all LORAN fixes to disc (Figures A.1.1 and A.1.2). Once all the 23 second-increment LORAN fixes are on disc, the data are run through the "KILSCAT" program, which filters, smooths, and interpolates the fixes. The new one minute-increment averaged data and the RADAR data are then run through the "OFFSET" program, to find the average offset and standard deviation between the LORAN and RADAR series (the "least squared" method is used - translation of center of mass). The average offset is used to add to all the LORAN fixes to generate the corrected or calibrated version of the navigation data. Track plots are then generated and if the plots do not show any gross errors, the corrected version will be taken as the final version of the navigation data. Preliminary plots can be run on the NORTH STAR and HOUSTON flatbed plotter using "MERC4" or on the NORTH STAR and CALCOMP drum plotter using "MERC5."

The data also may be transferred to an ALPHA-MICRO computer that is linked to another CALCOMP drum plotter. The ALPHA-MICRO may be used to transfer data to a disc file at the computer center using the "CCLINK" program. Otherwise, the only advantages to transferring data to the ALPHA-MICRO are its powerful text editor and the rapid "MERC8" plotting program to transfer final LORAN data to a disc file. "DSKCAS" and "CASDSK" programs are used. This disc file is accessed in the image processing steps of geometric rectification (Figure 5).

If data gaps on the ship navigation disc should ever occur, data must be typed in from the handwritten navigation log using the "MAKEFILE" program. "PLAYBACK" and "EDIT" are used to make any necessary corrections. Once the data is all complete on disc the procedure is as above.

A.1.2 Program descriptions

All the programs used in the processing are written in BASIC language for either the NORTH STAR HORIZON or ALPHA-MICRO microcomputers. Some of these programs are hybrids of Fortran versions written for the A/S-6 (OFFSET, MERC PLOT).

"NAVLOG," the navigation logging program, is used on ship to keep a record of LORAN fixes on disc and paper. Every 23 seconds, when the LORAN computes a fix, the computer acquires it and prints it out along with the corresponding time. The computer records 15 fixes on the disc at a time to preserve the disc drive mechanism. If the program is interrupted, then all the fixes in memory are recorded on disc instantly, the file is closed, and the program terminates. The following are possible program interruptions: overrunning user given time limits, power fluctuations, control-C command, or the LORAN goes bad.

"KILSCAT," which is used to attenuate LORAN scatter or noise, is a large and flexible program. It can find ship speed and direction, average an array of fixes, interpolate the averaged fixes to the minute, filter out bad fixes, and alert the user if data gaps of a given length are found. "KILSCAT" runs the fastest without using the printing options.

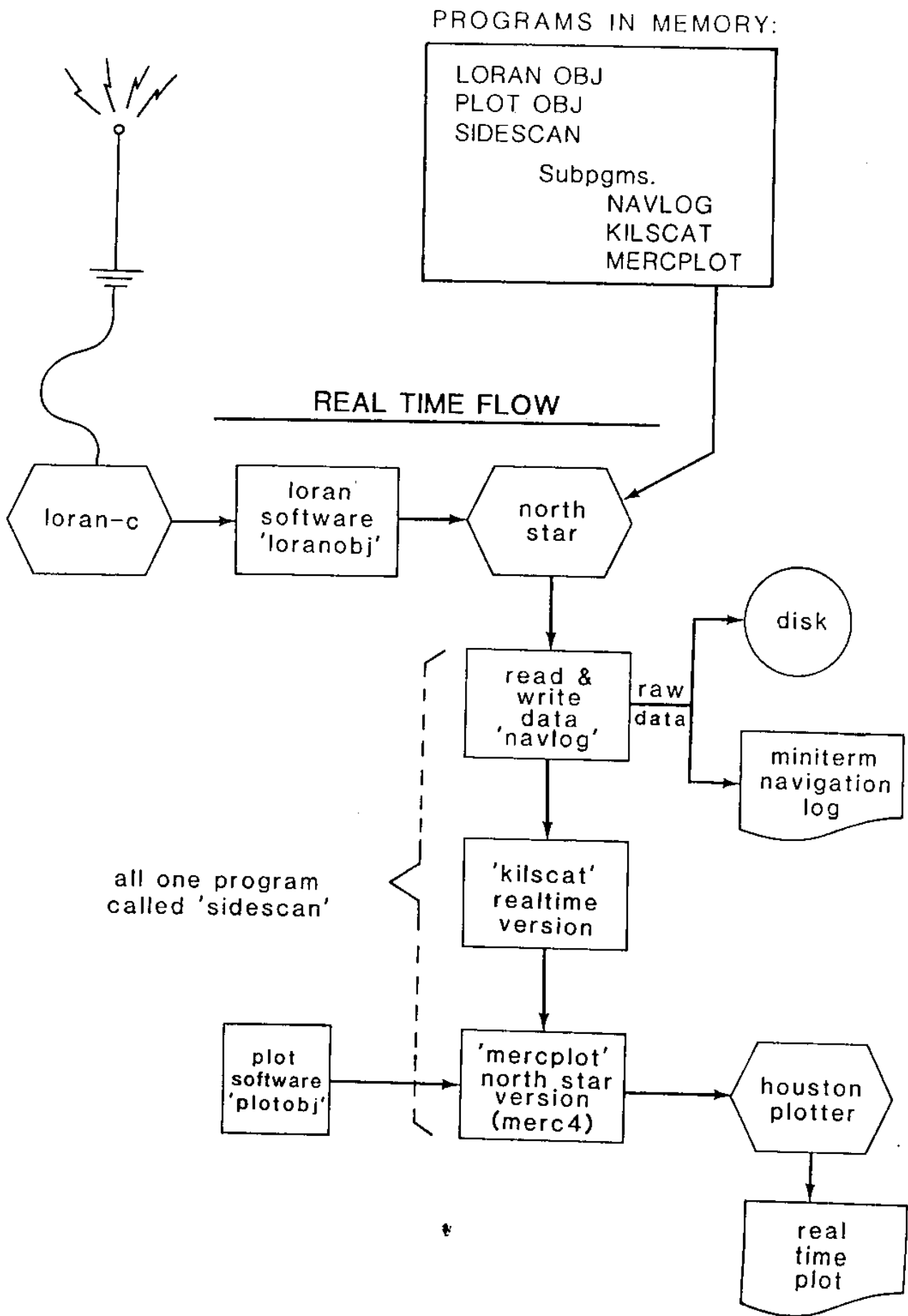
The calculated ship speed is found by comparing a new fix with a running averaged previous position. The distance between the two fixes is calculated and divided by the time difference. The calculated ship speed is compared to an upper limit ship speed (input parameter). If the calculated speed is more than the limit speed, the fix is thrown out and the next fix will be tested. A print out of the ship speed and direction is very useful for the process of producing mosaics. If there is a gap in the data exceeding a given length of time (input parameter), the user will be so notified and the program will automatically branch

to make a new running average with only the fixes after the time gap. The number of fixes averaged is also an input parameter. A linear running boxcar average is used to smooth the fixes.

Not only does "KILSCAT" smooth the fixes, but it reduces their number by two-thirds: i.e., instead of having three fixes per minute, there is only one fix per minute on the minute. Simple linear interpolation is used to obtain on-the-minute fixes.

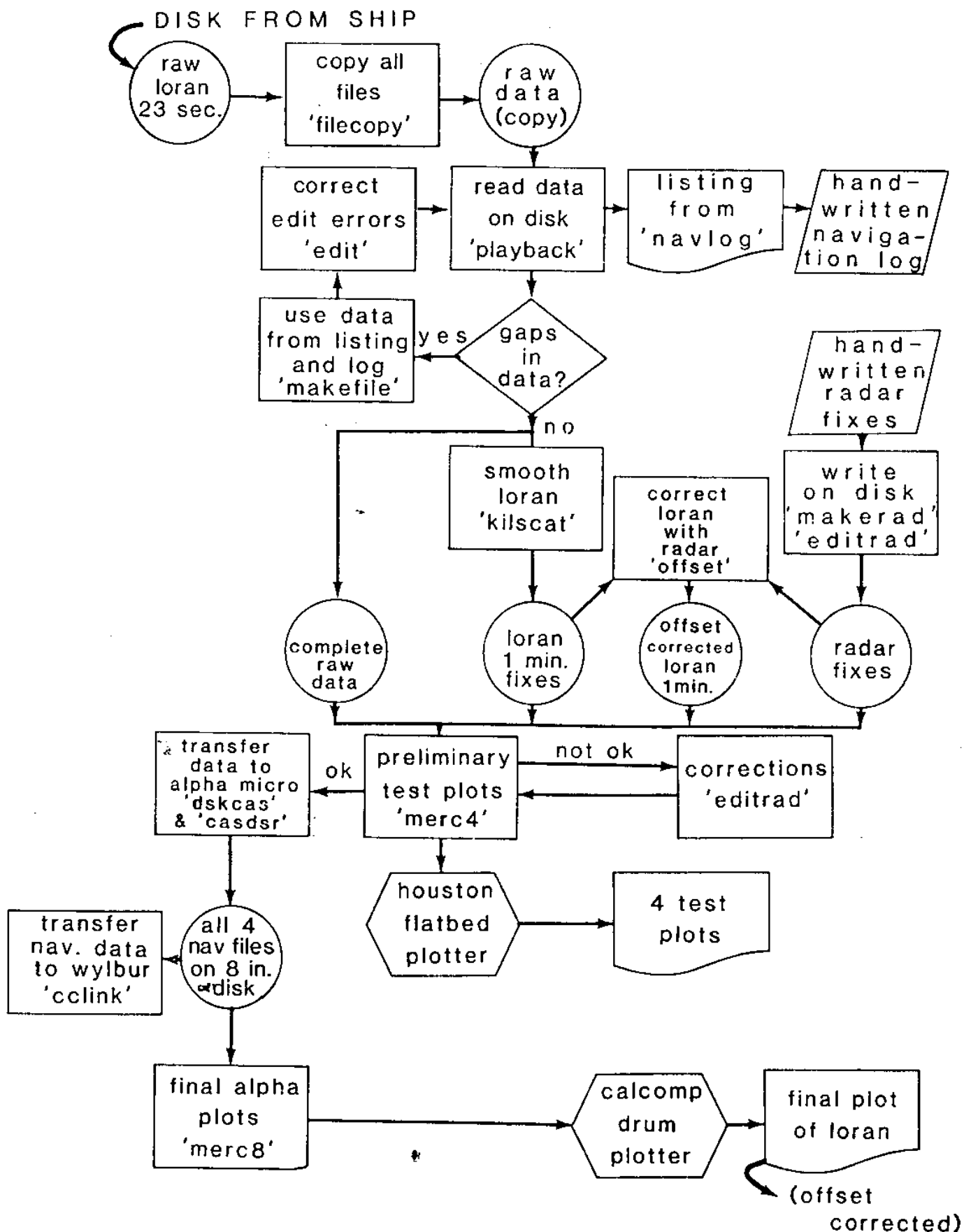
The RADAR fixes are usually more accurate than the LORAN fixes. "OFFSET" finds the average latitude-longitude offset between matching RADAR and LORAN fixes. This is done by subtracting the LORAN fix from the RADAR fix. It creates a new LORAN file by adding the average offset to the old LORAN fixes. The process is similar to sliding a map underneath undisturbed LORAN fixes.

Before running the "OFFSET" program, have ready the smoothed LORAN fixes from "KILSCAT" and the corresponding RADAR fixes from "MAKERAD." There are printing options that print out all RADAR and LORAN fixes. The final product of the program is RADAR-corrected LORAN fixes on disc.



NAVIGATION DATA PROCESSING

(ON NORTHSTAR AND ALPHA MICRO)



APPENDIX 2

Navigation processing in the laboratory: Pre-digital acquisition

by

Jaye E. UpDeGraff

A.2.1 Overview

On board the research vessel at sea, three types of fixes are taken to determine the ship's position. On the bridge, the ship's crew takes satellite fixes every few hours, and RADAR fixes on local landmarks every 15 to 30 minutes. In the lab, the scientific crew uses the LORAN-C receiver to obtain fixes every few minutes. On SSS-77-1 LORAN was recorded every 15 minutes, on subsequent cruises every 5 minutes. Because the frequency of fixes is much higher for RADAR and LORAN, these two types are employed in the navigation track positioning procedures.

The fix data recorded at sea must be transformed into formats usable in the computer programs employed. The hand-written data logs from each cruise must be keypunched onto cards. Each separate fix is typed onto a separate card, the cards (in chronological order) of a single cruise constitute a "data deck." The format used is termed FIXSE, and is one used by Woods Hole Oceanographic Institution. This format requires that the following information be keypunched on each card (for each data point, or navigation fix):

DATE-MONTH-YEAR-TIME (local)	cols. 1-10, Format (3I2,I4)
LATITUDE-DEGREES (+ north)	cols. 16-18, Format (I3)
LATITUDE-MINUTES (decimal)	cols. 19-25, Format (F7.2)
LONGITUDE-DEGREES (+ east)	cols. 26-30, Format (I5)
LONGITUDE-MINUTES (decimal)	cols. 31-37, Format (F7.2)
FIXCODE	cols. 42, Format (I1)

Types: dead reckoned	FIXCODE = 1
RADAR	= 3
LORAN-C	= 7
satellite fix	= 9

All of the pre-digital acquisition navigation was processed at the main UCSB computer center. Processing programs are written in Fortran-H, and plotting was done on a CALCOMP 30 inch drum plotter.

The original RADAR and LORAN navigation data decks are duplicated to preserve one copy each of the original navigation, and provide a second pair of decks to be used in refinement procedures.

The duplicate decks are then divided into sub-decks, based on the geographical area covered in the survey. This is done by plotting all the original data onto a 1:100,000 scale map, and then defining the areas in terms of where the survey tracks lay. The areas are of appropriate sizes to allow plots of the scale of 1:20,000 or 1:40,000 to be made using their boundaries. These sub-decks are labelled unambiguously for future reference and use.

To begin the navigation correction procedure, each pair of original RADAR and LORAN navigation is run through the TRACKS program and then plotted. The plot is analyzed for obvious mistakes, which are then corrected using dead-reckoning techniques and information provided by the ship's log. The corrected positions are keypunched onto cards in FIXSE format, and then inserted into the deck in place of the bad fix card. This deck is termed the "dead reckoned RADAR (or LORAN) deck."

The pair of dead-reckoned RADAR and LORAN decks are then run through the TRACKS program again, and another TRACK plot produced. This plot is analyzed again for bad fixes, and the same procedure is used to correct them, if it is necessary. These "corrected dead-reckoned decks" are then ready to be used in the OFFSET program.

The pair of "corrected dead-reckoned RADAR and LORAN decks" are run through the OFFSET program. (Only one area-pair of decks may be run at one time.) The OFFSET program will return an output listing as well as a new deck of LORAN cards, termed the "OFFSET-corrected LORAN deck."

The OFFSET-corrected LORAN deck is then run through the TRACKS program along with its corrected dead-reckoned RADAR deck in order to compare both navigation series (it is preferable to not have the RADAR fix points connected with line segments at this step). The plot returned is analyzed for any bad fixes. Any errors are corrected by dead-reckoning and use of the ship's log, and bad fix cards replaced by corrected fix cards.

This "dead-reckoned OFFSET-corrected" LORAN deck is next run through the DEDREK program. The DEDREK output is analyzed for flags indicating fixes with speed values and time increments greater than the anticipated maximums. Flagged fixes are examined against the ship's log of manuevers to determine if the computed values are valid. Invalid values for a fix are corrected by dead-reckoning using information from the ship's log. The corrected fixes are keypunched and inserted into the deck in place of the bad fixes. This deck with the corrected cards is the "final" LORAN deck. The final LORAN deck is lastly run through the TRACKS program, and a final plot is produced.

A.2.2 Program descriptions

The program TRACKS uses input navigation data card decks and CALCOMP plotter software to generate time-annotated navigation tracks on MERCATOR projection, which are plotted on a CALCOMP incremental drum plotter. The input navigation data cards must be in FIXSE format to use the TRACKS program. The program can plot various boundaries and scales plus plot various symbols at fixes to identify fix type.

The OFFSET program uses a dead-reckoned RADAR navigation data deck and a dead-reckoned LORAN navigation data deck of the same cruise, and mathematically corrects the offset LORAN fixes in reference to the RADAR fix positions. The offset is defined as the RADAR position minus the LORAN position. In the calculation and recording of LORAN fixes at sea, a systematic error occurs in the positioning of the fixes. The LORAN fixes are precise relative to each other, but may be geographically offset in their position. The position variation fluctuates in magnitude over large areas, but is constant over a small area (for example, the size of area covered in a separate survey). RADAR fixes do not have this type of position variation; they are accurate geographically and are therefore used as positions to which the LORAN fixes are calibrated. The LORAN track is calibrated in this way to produce an offset-corrected navigation track.

The DEDREK program calculates the speed, time and azimuth between two chronologically adjacent fixes. It then determines if any of the three values is greater than maximum values set on input. A notational flag is printed whenever the calculated values are greater than the given maximums. These flags key the interpreter to suspicious fixes.

APPENDIX 3

Analogue - Digital conversion of side-scan sonar data recorded at sea

by

Fred Ennerson

A.3.1 Digitization procedure

The digitization procedure involved performing A/D conversion on the sonar data recorded on a Racal 4-channel FM tape recorder. Two sonar channels and one timing (synch) channel were taped. The data channels (port and starboard) were processed using a different procedure than the sync channel. The data channels were first filtered at 500 Hz with a Krohn-hite model 3222 filter. This signal was then amplified to ± 10 volts (the range of the A/D hardware) using a Toshiba model SY-335 preamplifier and a Toshiba SC-355 amplifier. The resultant signal was then digitized. The sync channel was amplified and the syncpulse widened to three times its original length with a Hewlett Packard model #3300-A function generator. The reason for syncpulse enlargement was to ensure its detection during digitization.

Digitization was done using computers at the computer systems lab (CSL) of UCSB. These include a PDP 11/05 and 11/45. All three channels were digitized in sequential order (e.g., one sample from port, one from starboard, one from sync, one from port, starboard, sync, etc. . . .). The digitization frequency was 4,841 Hz for a sampling frequency of 1614 Hz per channel. The digitizer output was 13 bits in a 16 bit integer. The 13 bits consisted of 12 data bits and one sign bit, for a range of -2048 to +2048 grey levels.

Because of disk space limitations on the PDP 11/05 (the PDP 11/05 has three 2.1 M byte RK/05 disks) the data were digitized in small overlapping segments. After one segment was digitized and placed on the RK/05's, the data was then transferred, by means of a disk accessible to both the PDP 11/05 and 11/45, to the 11/45. Digitizing directly to the transfer disk was not done because the disk was not a dedicated disk and buffering proved impossible at the digitizing rate required.

A.3.2 Track reconstruction procedure

The first step of track reconstruction consisted of three parts: (1) separating the digital input file into three files (port, starboard, and sync) using internal buffers, (2) averaging the data by a running two sample cross-track average, (3) reducing the data from 2 bytes to 1 byte.

The second step of reconstruction involved manually finding the first five synchpulses using an interactive graphics system. The offset of the first synchpulse from the start of the file and the average time between synchpulses was calculated.

The third step of reconstruction was the creation of an image of equal line length for each channel. Based on the location of the first synchpulse and the average time between them, a computer program windowed around the estimated successive synchpulse time. The largest amplitude sample in this window was assumed to be the synchpulse. The program then repetitively windowed at each projected synchpulse time. When each synchpulse was found, the data channel (port or starboard) was demultiplexed and written out into a new file. The end of the data set (determined by synchpulse location) to the end of the standard line was buffered with zeros. A simple thresholding program to locate the synchpulses was not used because many of the noise spikes in the synch channel were of greater intensity than the synchpulse. If a noise spike near a synchpulse caused the windowing function to miss the next pulse, either the search window was enlarged or the offending noise spike was manually removed from the synch channel.

The fourth step of reconstruction was the combining of all of the small images into one large image of the entire track. Each track constitutes about 30 minutes of survey data. This was done by mosaicking (overlaying) the separate (sub)images into one large sequential image. For each pair of adjacent (sub)images a data line common to both was located. This was done by subtracting the first line of the second (sub)image from each of the last 100 lines of the first (sub)image. The line with the smallest amplitude difference was assumed to be the same line. The second image was added to the first at this point. In like manner, the third image was checked against the last 100 lines of the new image file and so on. The average difference of the match up lines was usually less than half the difference of any of the other lines. Once the entire image was reconstructed it was visually checked (by film-writing) to make sure it was processed correctly. If the check confirmed the image was correct, the image was then written onto tape for processing on the ITEL AS/6 at the main computer center.